Unfolding singularly perturbed Bogdanov points

Matthias Stiefenhofer *†

Fakultät für Mathematik, Universität Bielefeld
Postfach 100131, 33501 Bielefeld, Germany

Abstract

Bogdanov points that occur in the fast dynamics of singular perturbation problems are often encountered in applications; e.g. in the van der Pol–Duffing oscillator [18] or in the FitzHugh–Nagumo equation [3]. We analyze these points using a generic unfolding which ensures that the typical phenomena near a regularly perturbed Bogdanov point (saddle–nodes, Hopf points, periodic orbits, homoclinic orbits) carry over to Bogdanov points viewed in the context of singular perturbations. We combine analytical and numerical results to study the relations between these structures in the 3–dimensional unfolding space. In particular, the singularly perturbed homoclinic orbits can be analyzed after an appropriate blow of the singularly perturbed Bogdanov point using a technique from [3]. As indicated by numerical calculations the homoclinic orbits turn into homoclinic orbits of Shilnikov type that vanish presumably by a duck like explosion process [7], [10], [1], [9].

1 Introduction

Singular perturbation problems of the form

$$\begin{aligned} \dot u &= F(u,v) \in \mathbb{R}^n \\ \dot v &= \epsilon \cdot G(u,v) \in \mathbb{R}\ , \qquad 0 \le |\epsilon| \ll 1 \end{aligned} \tag{1.1}$$

represent one possibility of including the real parameter v of the u–system $\dot u = F(u,v)$ into the slow dynamics of the model. We investigate this perturbation process from $\epsilon = 0$ to $\epsilon \neq 0$ when the central u–system $\dot u = F(u,0)$ has a Bogdanov point; i.e. a stationary point with an algebraically double and geometrically simple eigenvalue zero [14]. We refer to a point of this kind as a singularly perturbed Bogdanov point of the (u,v)–system (1.1) if it satisfies additionally $G(u,0) = 0$. In this situation the well known technique of reducing to the 1–dimensional slow manifold defined by $F(u,v) = 0$ is impossible (cf. [11], [28]) and instead of enslaving the fast u–variables by the slow v–variable (cf. [16]) we may obtain new phenomena due to the equal coupling of all variables.

*supported by DFG Schwerpunktprogramm "Ergodentheorie, Analysis und effiziente Simulation dynamischer Systeme".

†current address: Hauptstraße 21 b, D–65760 Eschborn

The standard example of a singularly perturbed Bogdanov point is given by the travelling wave problem for the Fitzhugh–Nagumo equation [4], [15], [20]

$$\begin{aligned} \dot{u}_1 &= u_2 \\ \dot{u}_2 &= cu_2 + u_1(u_1 - a)(u_1 - 1) + v \\ \dot{v} &= \frac{\bar{\epsilon}}{c} \cdot (u_1 - \gamma v) . \end{aligned} \tag{1.2}$$

With $\epsilon = \bar{\epsilon}/c$ we obtain a system of the form (1.1) which has a singularly perturbed Bogdanov point at $(u, v, a, c) = 0$. In [3] we examined the travelling wave problem (1.2) with respect to homoclinic orbits near the singularly perturbed Bogdanov point.

In the current paper we perform two extensions. First, we extend the results from [3] to general systems of the form (1.1). For this purpose the notion of a generic unfolding of a singularly perturbed Bogdanov point is introduced. In that framework we do not restrict to homoclinic orbits, but investigate to a certain extent the unfolding structure of stationary points, periodic orbits, homoclinic orbits and invariant tori. We use analytical results from [10], [9], [3], [25], [26], numerical results from [18] and heuristic results from [24] that are mainly obtained from the model equation

$$\begin{aligned} \dot{u}_1 &= u_2 \\ \dot{u}_2 &= u_1^2 + u_1 u_2 + k u_2 + v \\ \dot{v} &= \epsilon \cdot (\lambda - u_1) \end{aligned} \tag{1.3}$$

which represents a generic (λ, k)–unfolding of the singularly perturbed Bogdanov point $(u, v, \lambda, k) = 0$. Other examples of singularly perturbed Bogdanov points appear in the context of van der Pol–Duffing oscillators [18], [24] and cell communication problems [13].

The paper is organized as follows. In section 2 the precise definitions are given and the resulting unfolding structure is stated. In section 3 a pretransformation is performed and in section 4 the periodic orbits and the invariant tori are investigated. Section 5 deals with homoclinic orbits obtained by blowing up the singularly perturbed Bogdanov point appropriately. This section contains the most technical part of the paper. We conclude the paper with some strange results and conjectures concerning a duck like behavior [7], [10], [1], [9] of homoclinic orbits of Shilnikov type motivated by numerical calculations.

2 The setting and the unfolding diagram

Consider a system of the form

$$\begin{aligned} \dot{u} &= F(u, v, p_1, p_2, \epsilon) \in \mathbb{R}^2 \\ \dot{v} &= \epsilon \cdot G(u, v, p_1, p_2, \epsilon) \in \mathbb{R} \end{aligned} \tag{2.1}$$

with

$$F^0 := F(0) = 0, \qquad \mathrm{tr}(F_u)^0 = 0, \qquad \det(F_u)^0 = 0, \qquad F_u^0 \neq 0 \in \mathbb{R}^{2,2}, \tag{2.2}$$

$$F_v^0 \notin \mathrm{R}[F_u^0], \qquad F_{uu}^0 \varphi_1^2 \notin \mathrm{R}[F_u^0] \qquad \text{with} \qquad \mathrm{N}[F_u^0] = \mathrm{span}\{\varphi_1\}, \tag{2.3}$$

$$G^0 := G(0) = 0, \qquad \begin{pmatrix} F_u & F_v \\ G_u & G_v \end{pmatrix}^0 \quad \text{is nonsingular,} \tag{2.4}$$

where tr, det and R, N denote the trace, determinant and the range, kernel of a matrix and the upper index '0' denotes evaluation at $(u, v, p_1, p_2, \epsilon) = (0, 0, 0, 0, 0)$. According to (2.2) the central u–system $\dot{u} = F(u, 0)$ has a Bogdanov point in the sense defined in the introduction. According to (2.3) the v–perturbation $\dot{u} = F(u, v, 0)$ of this system has a quadratic limit point with respect to v; i.e. the Bogdanov point is generically perturbed by the parameter v. In the next step, the parameter v of the u–system $\dot{u} = F(u, v, 0)$ is included into the dynamics of the (u, v)–system (2.1) according to $\dot{v} = \epsilon G(u, v, 0, 0, \epsilon)$ where this dynamical unfolding is characterized by (2.4); i.e. the F–null cline defined by $F(u, v, 0) = 0 \in \mathbb{R}^2$ and the surface defined by $G(u, v, 0) = 0 \in \mathbb{R}$ intersect transversally in the Bogdanov point $(u, v) = 0$.

We call a point $(u, v, \epsilon) = 0$ which satisfies (2.2)–(2.4) a *singularly perturbed Bogdanov point* of the system

$$\begin{aligned} \dot{u} &= F(u, v, 0, 0, \epsilon) \\ \dot{v} &= \epsilon \cdot G(u, v, 0, 0, \epsilon) \ . \end{aligned} \tag{2.5}$$

Summing up we investigate a certain dynamical unfolding of a Bogdanov point of the u–system which satisfies $G = 0$ and some additional nondegeneracy conditions.

Next we turn to the assumptions concerning the (p_1, p_2)–parameter unfolding of system (2.5). Apart from the basic condition $(F, G)^0 = 0$ the central point $(u, v, \epsilon) = 0$ satisfies the two degeneracy conditions $\mathrm{tr}(F_u)^0 = 0$ and $\det(F_u)^0 = 0$. Hence it seems appropriate to examine a singularly perturbed Bogdanov point within an unfolding of two parameters $p = (p_1, p_2)$. The corresponding nondegeneracy condition of this unfolding is determined with the help of the defining equation

$$H(u, v, p_1, p_2) := \begin{pmatrix} F(u, v, p_1, p_2, 0) \\ G(u, v, p_1, p_2, 0) \\ \det(F_u)(u, v, p_1, p_2, 0) \\ \mathrm{tr}(F_u)(u, v, p_1, p_2, 0) \end{pmatrix} = 0, \qquad H : \mathbb{R}^5 \to \mathbb{R}^5 \ . \tag{2.6}$$

Then the nondegeneracy condition reads

$$H'(0) = \begin{pmatrix} F_u & F_v & F_{p_1} & F_{p_2} \\ G_u & G_v & G_{p_1} & G_{p_2} \\ \det_u(F_u) & \det_v(F_u) & \det_{p_1}(F_u) & \det_{p_2}(F_u) \\ \mathrm{tr}_u(F_u) & \mathrm{tr}_v(F_u) & \mathrm{tr}_{p_1}(F_u) & \mathrm{tr}_{p_2}(F_u) \end{pmatrix}^0 \in \mathbb{R}^{5,5} \quad \text{is nonsingular;} \tag{2.7}$$

i.e. the point $(u, v, p_1, p_2) = 0$ must be a regular solution of the defining equation (2.6). We call a (p_1, p_2)–unfolding of the system (2.5) which satisfies (2.7) a *generic unfolding of a singularly perturbed Bogdanov point.* This condition simply ensures that the singularly perturbed Bogdanov point $(u, v, \epsilon) = 0$ of system (2.5) is unique within the unfolded system (2.1).

With $(p_1,p_2) = (a,c)$ and $(p_1,p_2) = (\lambda,k)$ respectively, the travelling wave problem (1.2) and the model equation (1.3) satisfy the conditions (2.2)–(2.4) and (2.7). Another example is given by the van der Pol–Duffing oscillator [18]

$$\begin{aligned} \dot{u}_1 &= p_2 u_2 - u_1^3 + 3u_1 - p_1 \\ \dot{u}_2 &= u_1 - 2u_2 + v \\ \dot{v} &= \epsilon \cdot (u_2 - v) \end{aligned} \tag{2.8}$$

which can be interpreted as a generic (p_1,p_2)–unfolding of each of the two singularly perturbed Bogdanov points

$$(u_1,\ u_2,\ v,\ p_1,\ p_2) = \left(\pm\frac{1}{\sqrt{3}}\,,\ \pm\frac{1}{\sqrt{3}}\,,\ \pm\frac{1}{\sqrt{3}}\,,\ \mp\frac{4}{3\sqrt{3}}\,,\ -4 \right). \tag{2.9}$$

Further examples can be found in [24] where cell communication problems from [13] are studied.

Our aim is to determine the unfolding structure of the general system (2.1) in the (p_1,p_2,ϵ)–parameter space. For this purpose we first determine the unfolding structure of the u–system $\dot{u} = F(u,v,p_1,p_2,0)$ and then we perform the singular perturbation from $\epsilon = 0$ to $\epsilon \neq 0$; i.e. we include the generic parameter v into the dynamics of the system.

Now the regularity of $H'(0)$ ensures that the singularly perturbed Bogdanov point lies at the intersection of the curves defined by

$$[F,\ G,\ \det(F_u)](u,v,p_1,p_2,0) = 0 \qquad \text{and} \qquad [F,\ G,\ \mathrm{tr}(F_u)](u,v,p_1,p_2,0) = 0. \tag{2.10}$$

In the next section it is shown that these curves give rise to saddle–node and Hopf points of the u–system $\dot{u} = F(u,v,p_1,p_2,0)$ which satisfy $G(u,v,p_1,p_2,0) = 0$. Moreover, we shall see that a curve of homoclinic base points (the steady states to which the homoclinic orbits converge) of the system $\dot{u} = F(u,v,p_1,p_2,0)$ with $G(u,v,p_1,p_2,0) = 0$ emanates from the singularly perturbed Bogdanov point. In analogy to the definition of a singularly perturbed Bogdanov point we refer to these phenomena as *singularly perturbed saddle–nodes, Hopf points and homoclinic base points* respectively. In this sense the assumptions (2.2)–(2.4) and (2.7) guarantee that the typical phenomena near a regularly perturbed Bogdanov point [14] carry over to Bogdanov points viewed in the context of singular perturbations.

In diagram (a) of Fig.1 we show the general location of these singularly perturbed points in the (p_1,p_2)–plane as they occur for the system (2.1) in generic cases.

The singularly perturbed Hopf points HP_s and the singularly perturbed homoclinic base points Ho_s terminate at the singularly perturbed Bogdanov point BP_s, whereas the singularly perturbed saddle-nodes SN_s are passing through this point. The points HP_s and Ho_s occur on different sides of the curve of SN_s points. In general, these three curves meet transversally at $(p_1,p_2) = 0$. For graphical reasons the points SN_s are drawn along the p_2-axis.

In case of the FitzHugh–Nagumo equation (1.2) we obtain diagram (b) in Fig.1; i.e. the singularly perturbed homoclinic orbits and the singularly perturbed Hopf points are positioned on the a–axis. In particular they do not meet transversally at the origin. This is a degenerate situation which results from the fact that the central u–system $\dot{u}_1 = u_2$, $\dot{u}_2 = -u_1^2 + u_1^3$ of the FitzHugh–Nagumo equation is Hamiltonian. We return to this situation in section 5.

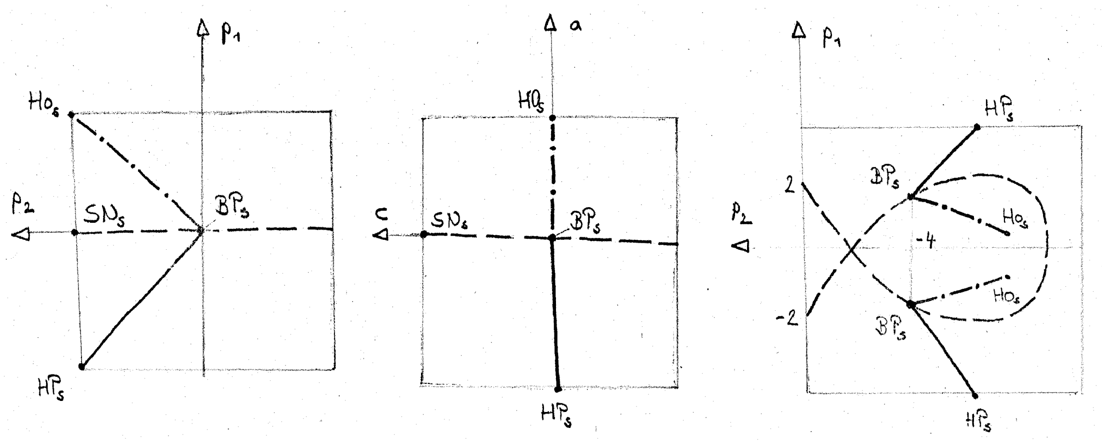

(a) (b) (c)

Figure 1: The singularly perturbed points at $\epsilon = 0$: (a) Standard, (b) FitzHugh–Nagumo, (c) van der Pol–Duffing.

Diagram (c) in Fig.1 shows the singularly perturbed points of the van der Pol–Duffing oscillator (2.8) which represents an example of two times the standard case. Further examples of the standard case are given by the model equation (1.3) and the cell communication problems studied in [24].

The singularly perturbed saddle–node and Hopf points in the three systems (1.3), (1.2) and (2.8) can be given explicitly. In general it is only possible to calculate the derivative of these curves at the singularly perturbed Bogdanov point (cf. sections 3 and 4). The derivative of the curve of singularly perturbed homoclinic base points Ho_s is derived in section 5.

The following are the parameter values of the singularly perturbed points. In case of the model equation (1.3) we obtain

$$\begin{array}{llll} SN_s: & (\lambda\,,k) &=& (0\,,k)\;, & k \neq 0 \\ HP_s: & (\lambda\,,k) &=& (\lambda\,,-\lambda)\;, & \lambda < 0 \\ Ho_s: & (\lambda\,,k) &=& (\lambda\,,k(\lambda))\;, & \lambda > 0 \quad \text{with} \quad \frac{d}{d\lambda}k(\lambda) \to \frac{5}{7} \quad \text{as} \quad \lambda \to 0 \end{array}$$

(cf. diagram (a) in Fig.1 with $p_1 = \lambda$, $p_2 = k$). In case of the FitzHugh–Nagumo equation (1.2) the singularly perturbed points occur at

$$\begin{array}{lllll} SN_s: & (a\,,c) &=& (0\,,c)\;, & c \neq 0 \\ HP_s: & (a\,,c) &=& (a\,,0)\;, & a < 0 \\ Ho_s: & (a\,,c) &=& (a\,,0)\;, & a > 0 \end{array}$$

(cf. diagram (b) in Fig.1) and, finally, for the van der Pol–Duffing oscillator (2.8) we have

$$\begin{array}{lll} SN_s: & (p_1\,,p_2) = (5s^3 - 3s\,,6s^2 - 6)\;, & s \in (-1,1) \setminus \{\pm\frac{1}{\sqrt{3}}\} \\ HP_s: & (p_1\,,p_2) = (\pm(p_2 + \frac{8}{3})/\sqrt{3}\,,p_2)\;, & p_2 < -4 \\ Ho_s: & (p_1\,,p_2) = (p_1^{\mp}(p_2)\,,p_2)\;, & \text{with} \quad \frac{d}{dp_2}p_1^{\mp}(p_2) \to \mp\frac{1}{5\sqrt{3}} \quad \text{as} \quad p_2 \to -4 \end{array}$$

(cf. diagram (c) in Fig.1). The curve SN_s is globally parametrized by the external parameter s such that the singularly perturbed Bogdanov points BP_s occur at $s = \pm 1/\sqrt{3}$.

Next we perturb these basic structures from $\epsilon = 0$ to $\epsilon \neq 0$. Concerning this process note that the linearization of the system (2.1) at the central point reads

$$\begin{pmatrix} F_u^0 & F_v^0 \\ 0 & 0 \end{pmatrix} \in \mathrm{IR}^{3,3} \qquad \text{with} \qquad \mathrm{tr}(F_u)^0 = 0 \qquad \text{and} \qquad \det(F_u)^0 = 0 \tag{2.11}$$

implying an eigenvalue zero of multiplicity three. Hence without considering the singular perturbation character of the system (2.1) we are confronted with a highly degenerate situation. On the other hand the assumption (2.4) implies

$$\det(\begin{pmatrix} F_u & F_v \\ \epsilon G_u & \epsilon G_v \end{pmatrix})(u, v, p_1, p_2, \epsilon) \;=\; \epsilon \cdot \det(\begin{pmatrix} F_u & F_v \\ G_u & G_v \end{pmatrix})(u, v, p_1, p_2, \epsilon) \;\neq 0 \tag{2.12}$$

for $\epsilon \neq 0$; i.e. the threefold eigenvalue zero splits completely into eigenvalues different from zero when passing from $\epsilon = 0$ to $\epsilon \neq 0$. In particular there exist no saddle–node or Bogdanov points for $\epsilon \neq 0$ which simplifies the unfolding problem considerably.

Now in case of the model equation (1.3) (use $p_1 = \lambda$, $p_2 = k$) a combination of analytical, numerical and heuristical results yields the unfolding structures depicted in diagram (a) of Fig.2. Note that this diagram represents the ϵ–extension of Fig.1 diagram (a). The numerical calculations were performed with [8] and programs from [21].

Roughly speaking, this diagram is characterized by three surfaces: A surface of Hopf points HP, a surface of Naimark–Sacker points NP and a surface of homoclinic orbits (or homoclinic base points) Ho. The surface of Hopf points connects the singularly perturbed saddle–nodes SN_s and the singularly perturbed Hopf points HP_s. In addition the points HP_s give rise to the surface NP of Naimark–Sacker points; i.e. we obtain a surface of periodic orbits with a pair of complex–conjugate Floquet multipliers on the unit circle which implies generically the existence of a 3-dimensional domain of invariant tori near the surface of Naimark–Sacker points (cf. [14]).

The surface NP terminates at the curve NP_{-1} of periodic orbits with double Floquet multiplier -1. On the other hand we obtain the threefold Floquet multiplier 1 along the curve of HP_s–points at $\epsilon = 0$. Hence during variation along the dotted line [a] the two Floquet multipliers different from 1 are passing along the unit circle from 1 to -1 as indicated in diagram (b). This leads to curves of NP–points in diagram (a) with fixed Floquet multipliers on the unit circle. These curves approach the central point $(p_1, p_2, \epsilon) = 0$. As an example, the curve of NP–points with fixed Floquet multipliers $\pm i$ is indicated by NP_i.

Passing to the study of maps via a Poincaré section the points NP_{-1} and NP_i are known as 1 : 2 and 1 : 4 resonances, respectively (see [19] for their unfolding). We conclude that the central (u, v)–system

$$\begin{aligned} \dot{u} &= F(u, v, 0, 0, 0) \\ \dot{v} &= 0 \end{aligned} \tag{2.13}$$

at $(p_1, p_2, \epsilon) = 0$ gives rise to completely different kinds of periodic orbits. The complete picture is unknown. Our suggestion is that the periodic orbits along NP_i or NP_{-1} are

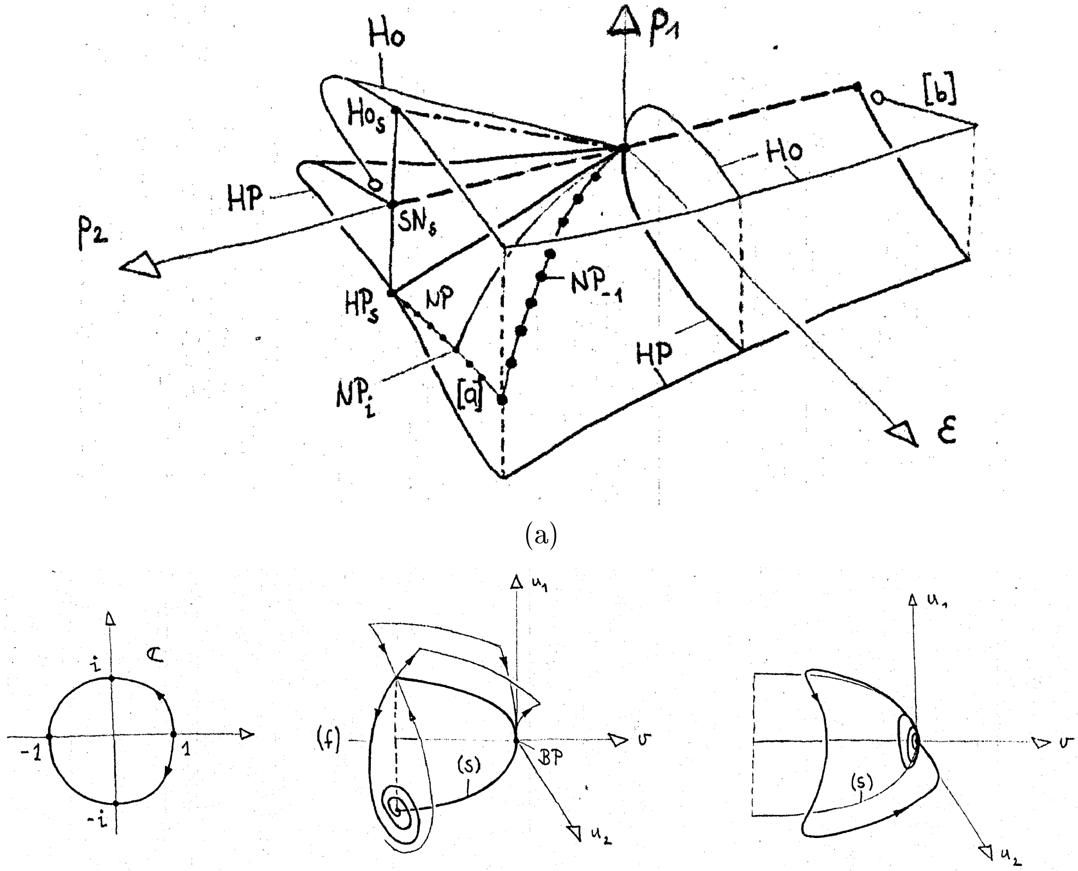

(b) (c) (d)

Figure 2: (a) (p_1, p_2, ϵ)–unfolding diagram, (b) Floquet multipliers along [a], (c) a singular periodic orbit in the (u, v)–phase space of the central system (2.13), (d) a typical homoclinic orbit of Shilnikov type near the border line of open circles.

starting in a duck like manner from a singular periodic orbit (cf. [9]) of the system (2.13) composed of fast (f) and slow motions (s) as indicated in the (u, v)–phase diagram (c). Note that the central (u, v)–system (2.13) inherits the continuum of stationary points (s) which consists of saddles and oscillating sinks (with respect to the fast u–dynamics) separated by a Bogdanov point BP at $v = 0$.

Next we turn to the surface of homoclinic orbits Ho in diagram (a) that bifurcates from the singularly perturbed base points Ho_s at $\epsilon = 0$. In general this bifurcation is not smooth in ϵ; i.e. the surface has an edge along the curve of Ho_s–points at $\epsilon = 0$ (cf. section 5.1).

Further, as indicated by the open circles the surface Ho is bordered by a curve through the central point $(p_1, p_2, \epsilon) = 0$ along which the homoclinic orbits vanish presumably by a duck like blow–up. More precisely, along the curve [b] we expect that the homoclinic orbits turn first into homoclinic orbits of Shilnikov type [14] and finally blow–up along the continuum of stationary points (s) of the central system (2.13) as indicated in diagram (d). Some additional features of this explosion process are described in section 5.2.

Now we return to the general system (2.1) under the assumptions (2.2)–(2.4) and (2.7). We expect that the structures in Fig.2 of the model equation (1.3) represent a typical unfolding diagram of singularly perturbed Bogdanov points in a generic situation. Some aspects of this claim are verified analytically in the next sections. Moreover, numerical calculations for the van der Pol–Duffing oscillator (2.8) (cf. [18]) and the cell communication problems in [24] confirm this conjecture.

We notice, however, that the Hamiltonian case (1.2) of the FitzHugh–Nagumo equation exhibits some special features (cf. diagram (b) in Fig.1). Therefore, we close this section with some remarks on deformations of the unfolding picture that might occur in specific examples.

First, the surfaces in Fig.2 diagram (a) may be deformed diffeomorphically as usual; i.e. we are only interested in structures that are not destroyed by diffeomorphic parameter transformations. For example, the folds of Hopf and homoclinic base points shown in diagram (a) may vanish under an appropriate change of the parameters. On the other hand the transversal intersections of manifolds of singularly perturbed points represent diffeomorphic invariants.

Secondly, a singular perturbation problem of the form (2.1) contains at $(p_1, p_2, \epsilon) = 0$ a continuum of stationary points in the (u, v)–phase space defined by $F(u, v, 0) = 0$ (cf. diagram (c) in Fig.2). Even in the weak sense of algebraic singularity theory [12] this leads to a completely degenerate situation, i.e. a codim $= \infty$ situation occurs, so that we can not hope to grasp all possible phenomena near a singularly perturbed Bogdanov point with the help of a certain normal form. In this sense singular perturbation problems do not fit into the framework of universal unfoldings which are based on the fact that higher order derivatives do not change the qualitative behavior of the system.

Nevertheless, every singularly perturbed Bogdanov point with a generic unfolding will show the properties that are completely determined by the derivatives involved in (2.2)–(2.4) and (2.7). But the phenomena which depend on higher derivatives will change for different singularly perturbed Bogdanov points. In spite of this principal lack of completeness which occurs in singular perturbation problems we hope that our results grasp the essential features of singularly perturbed Bogdanov points.

3 A pretransformation

First we perform a pretransformation of the system (2.1) under the slightly weaker assumption (cf. (2.7))

$$\operatorname{rank}\left(\begin{pmatrix} F_u & F_v & F_{p_1} & F_{p_2} \\ G_u & G_v & G_{p_1} & G_{p_2} \\ \det_u(F_u) & \det_v(F_u) & \det_{p_1}(F_u) & \det_{p_2}(F_u) \end{pmatrix}^0 \right) = 4 \ . \tag{3.1}$$

According to the assumption (2.2) the point $u = 0$ is a Bogdanov point of the system $\dot{u} = F(u, 0)$. Hence there exist $\varphi_2, \psi_1, \psi_2 \in \mathbb{R}^2 \setminus \{0\}$ with

$$F_u^0 \varphi_2 = \varphi_1 \ , \qquad \psi_2^T F_u^0 = 0 \ , \qquad \psi_1^T F_u^0 = \psi_2^T \ , \qquad \psi_i^T \varphi_j = \delta_{ij} \ . \tag{3.2}$$

Further the system $\dot{u} = F(u, v, 0)$ has a quadratic limit point with respect to v (cf. (2.3)). Thus, there exist a surface of quadratic limit points $(u, v)^L(p_1, p_2, \epsilon)$ of $\dot{u} = F(u, v, p_1, p_2, \epsilon)$

and smooth tangent vectors $\phi_1(p_1, p_2, \epsilon)$ such that $(u,v)^L(0) = 0$, $\phi_1(0) = \varphi_1$. This follows from the implicit function theorem applied to the equation $[F, \det(F_u)][u, v, p_1, p_2, \epsilon] = 0$. We obtain the identity $[F, \det(F_u)^0][(u,v)^L(p_1, p_2, \epsilon), p_1, p_2, \epsilon] = 0$ and differentiation with respect to $p = (p_1, p_2)$ yields

$$\begin{pmatrix} u_p^L \\ v_p^L \end{pmatrix}(0) \;=\; -\begin{pmatrix} F_u^0 & F_v^0 \\ \det_u(F_u)^0 & \det_v(F_u)^0 \end{pmatrix}^{-1} \cdot \begin{pmatrix} F_p^0 \\ \det_p(F_u)^0 \end{pmatrix} \tag{3.3}$$

where the regularity of the matrix follows from (2.2), (2.3). Next we plug the limit points into the equation $G = 0$; i.e. we analyze $G[(u,v)^L(p,\epsilon), p, \epsilon] = 0$. At $(p, \epsilon) = 0$ we have $G[(u,v)^L(0), 0] = G^0 = 0$ and (3.1), (3.3) imply

$$\frac{d}{dp}\, G[(u,v)^L(0), 0] \;=\; (G_u^0, G_v^0) \cdot \begin{pmatrix} u_p^L \\ v_p^L \end{pmatrix}(0) \;+\; G_p^0 \;\neq\; (0,0). \tag{3.4}$$

Without loss of generality we may assume $\frac{d}{dp_1} G[(u,v)^L(0), 0] \neq 0$. Hence there exists a unique smooth function $p_1(p_2)$ satisfying $p_1(0) = 0$ and

$$G[(u,v)^L(p_1(p_2), p_2, 0), p_1(p_2), p_2, 0] \;=\; 0\;; \tag{3.5}$$

i.e. within the 2–dimensional surface of limit points $(u,v)^L(p,0)$ of the u–system $\dot{u} = F(u, v, p, 0)$ we obtain a curve of limit points which satisfies $G = 0$. Now we define the matrices $\phi(p, \epsilon) := [\phi_1(p,\epsilon), \varphi_2] \in \mathbb{R}^{2,2}$ and consider the transformation

$$\begin{aligned} p_1 &= p_1(k) \;+\; \lambda \\ p_2 &= k \\ u &= u^L[p_1(k) + \lambda, k, \epsilon] \;+\; \phi[p_1(k) + \lambda, k, \epsilon] \cdot x \;=:\; u(x, \lambda, k, \epsilon) \\ v &= v^L[p_1(k) + \lambda, k, \epsilon] \;+\; y =:\; v(y, \lambda, k, \epsilon)\;; \end{aligned} \tag{3.6}$$

i.e. the limit points are moved to the origin of phase space, the limit points which satisfy $G = 0$ at $\epsilon = 0$ are positioned on the k–axis and a linear normalisation of the u–components is performed. We arrive at the system

$$\begin{aligned} \dot{x} &= \phi^{-1}[p_1(k) + \lambda, k, \epsilon] \cdot F[u(x, \lambda, k, \epsilon), v(y, \lambda, k, \epsilon), p_1(k) + \lambda, k, \epsilon] \\ &=: f(x, y, \lambda, k, \epsilon) \\ \dot{y} &= \epsilon \cdot G[u(x, \lambda, k, \epsilon), v(y, \lambda, k, \epsilon), p_1(k) + \lambda, k, \epsilon] \\ &=: \epsilon \cdot g(x, y, \lambda, k, \epsilon) \end{aligned} \tag{3.7}$$

which satisfies

$$f(0, 0, \lambda, k, \epsilon) \;\equiv\; 0, \qquad f_{x_1}(0, 0, \lambda, k, \epsilon) \;\equiv\; 0, \qquad g(0, 0, 0, k, 0) \;\equiv\; 0,$$

$$\begin{pmatrix} f_x & f_y \\ g_x & g_y \end{pmatrix}^0 = \begin{pmatrix} 0 & 1 & \psi_1^T F_v^0 \\ 0 & 0 & \psi_2^T F_v^0 \\ G_u^0 \varphi_1 & G_u^0 \varphi_2 & G_v^0 \end{pmatrix} \quad \text{nonsingular,}$$

$$
\begin{aligned}
g_\lambda^0 &= (G_u \quad G_v \quad G_{p_1})^0 \cdot \begin{pmatrix} u_{p_1}^L \\ v_{p_1}^L \\ 1 \end{pmatrix}(0) \neq 0, \\
p_1'(0) &= -\frac{1}{g_\lambda^0}\,(G_u \quad G_v \quad G_{p_2})^0 \cdot \begin{pmatrix} u_{p_2}^L \\ v_{p_2}^L \\ 1 \end{pmatrix}(0),
\end{aligned}
\tag{3.8}
$$

$$
\begin{aligned}
(f_{x_1x_1} \quad f_{x_1x_2})^0 &= \begin{pmatrix} \psi_1^T \\ \psi_2^T \end{pmatrix} \cdot (F_{uu}^0\varphi_1^2 \quad F_{uu}^0\varphi_1\varphi_2) \qquad \text{with} \qquad f_{2x_1x_1}^0 \neq 0, \\
(f_{2x_2\lambda} \quad f_{2x_2k})^0 &= (\mathrm{tr}_u(F_u) \quad \mathrm{tr}_v(F_u) \quad \mathrm{tr}_p(F_u))^0 \cdot \begin{pmatrix} u_p^L \\ v_p^L \\ I_2 \end{pmatrix}(0) \cdot \begin{pmatrix} 1 & p_1'(0) \\ 0 & 1 \end{pmatrix}.
\end{aligned}
$$

The last identity follows after a lengthy but straightforward calculation using (3.2) and

$$
\begin{aligned}
F_u[(u,v)^L(p,0),p,0] \cdot \phi_1(p,0) &= 0, \\
\mathrm{tr}_a(F_u)^0 = \psi_1^T F_{ua}^0 \varphi_1 + \psi_2^T F_{ua}^0 \varphi_2 \qquad &\text{for} \qquad a = u_1, u_2, v, p_1, p_2\,.
\end{aligned}
\tag{3.9}
$$

Moreover we obtain from (3.3) and (3.8) after some calculations

$$
\begin{aligned}
f_{2x_2k}^0 &= -\frac{1}{g_\lambda^0}\cdot \det\Big(\begin{pmatrix} \mathrm{tr}_u(F_u) & \mathrm{tr}_v(F_u) \\ G_u & G_v \end{pmatrix}^0 \cdot \begin{pmatrix} u_p^L \\ v_p^L \end{pmatrix}(0) + \begin{pmatrix} \mathrm{tr}_p(F_u) \\ G_p \end{pmatrix}^0 \Big) \\
&= \frac{1}{g_\lambda^0}\cdot \det\Big(\begin{pmatrix} \mathrm{tr}_u(F_u) & \mathrm{tr}_v(F_u) \\ G_u & G_v \end{pmatrix} \begin{pmatrix} F_u & F_v \\ \det_u(F_u) & \det_v(F_u) \end{pmatrix}^{-1} \begin{pmatrix} F_p \\ \det_p(F_u) \end{pmatrix} \\
&\quad - \begin{pmatrix} \mathrm{tr}_p(F_u) \\ G_p \end{pmatrix} \Big)^0 .
\end{aligned}
\tag{3.10}
$$

Note that the defining condition (2.7) of a generic unfolding implies $f_{2x_2k}^0 \neq 0$, whereas the weaker assumption (3.1) of this section does not exclude the case $f_{2x_2k}^0 = 0$. The homoclinic orbits of the systems (2.1) and (3.7) depend heavily on this coefficient. In the analysis of singularly perturbed saddle–node and Hopf points (cf. section 4) we restrict to $f_{2x_2k}^0 \neq 0$ whereas the singularly perturbed homoclinic orbits are investigated for $f_{2x_2k}^0 \neq 0$ and $f_{2x_2k}^0 = 0$ as well (cf. section 5). In case of $f_{2x_2k}^0 = 0$ we require further coefficients to be different from zero.

4 Singularly perturbed saddle–node and Hopf points

In this section we prove the existence and location of singularly perturbed saddle–nodes SN_s and Hopf points HP_s as depicted in Fig.1. The results are stated for the transformed system (3.7). It is always obvious how to transfer these results from the (λ, k, ϵ)–space into the (p_1, p_2, ϵ)–parameter space of the original system (2.1). The p_1–axis and the p_2–axis in Fig.1, Fig.2 are often referred to as λ–axis and k–axis respectively.

First we verify curves of saddle–node and Hopf points of the x–system $\dot{x} = f(x, y, \lambda, k, 0)$ which satisfy $g(x, y, \lambda, k, 0) = 0$ in addition. Then we state the known results about the unfolding structure of such points. We refer to [7], [10], [1], [9], [25] in case of singularly perturbed saddle–nodes and to [26] in case of singularly perturbed Hopf points.

4.1 Unfolding singularly perturbed saddle–nodes

According to the transformation (3.6) the points $(x, y, \lambda, k) = (0, 0, 0, k)$ represent quadratic limit points with respect to y of the x–system $\dot{x} = f(x, y, \lambda, k, 0)$ that satisfy $g(0, 0, 0, k, 0) = 0$. The linearization of the system (3.7) at these points is given by (cf. (3.8))

$$\begin{pmatrix} f_x & f_y \\ 0 \cdot g_x & 0 \cdot g_y \end{pmatrix} (0, k, 0) \;=\; \begin{pmatrix} 0 & f_{1x_2} & f_{1y} \\ 0 & f_{2x_2} & f_{2y} \\ 0 & 0 & 0 \end{pmatrix} (0, k, 0) \tag{4.1}$$

with $f_{1x_2}(0, k, 0) = 1 + O(k)$, $f_{2x_2}(0, k, 0) = f^0_{2x_2k} \cdot k + O(k^2)$, $f_{2y}(0, k, 0) \neq 0$ and $f^0_{2x_2k} \neq 0$ due to the assumption of a generic unfolding. We obtain for every $k \neq 0$ the algebraically double and geometrically simple eigenvalue zero with generalized eigenspace $\mathrm{span}\{(1, 0, 0)^T, (0, f_{2y}(0, k, 0), -f_{2x_2}(0, k, 0))^T\}$ and hence there exists for every $k \neq 0$ a local center manifold which can be parametrized by the coordinates (x_1, y) and the parameters (λ, k, ϵ) (cf. [23]). Strictly speaking there exists a smooth function $x_2(x_1, y, \lambda, k, \epsilon)$, $k \neq 0$ such that the surface

$$(x_1 \;,\; x_2 \;,\; y) \;=\; (x_1 \;,\; x_2(x_1, y, \lambda, k, \epsilon) \;,\; y) \;, \qquad k \;\neq\; 0 \tag{4.2}$$

remains invariant under the flow of system (3.7) in the (x_1, x_2, y)–phase space. At $(y, \lambda, \epsilon) = 0$ we obtain the x_1–expansion

$$x_2(x_1, 0, 0, k, 0) \;=\; -\frac{1}{2}\,\frac{f_{2x_1x_1}}{f_{2x_2}}(0, k, 0) \cdot x_1^2 \;+\; O(x_1^3), \qquad k \;\neq\; 0 \;. \tag{4.3}$$

The dynamics on the invariant surface is determined by

$$\begin{aligned} \dot{x}_1 \;&=\; f_1(x_1 \;,\; x_2(x_1, y, \lambda, k, \epsilon) \;,\; y \;,\; \lambda \;,\; k \;,\; \epsilon) \quad &=:\quad & \bar{f}(x_1, y, \lambda, k, \epsilon) \\ \dot{y} \;&=\; \epsilon \cdot g(x_1 \;,\; x_2(x_1, y, \lambda, k, \epsilon) \;,\; y \;,\; \lambda \;,\; k \;,\; \epsilon) \quad &=:\quad & \epsilon \cdot \bar{g}(x_1, y, \lambda, k, \epsilon) \end{aligned} \tag{4.4}$$

and we have again the singular perturbation form (1.1). At $(x_1, y, \lambda, k) = (0, 0, 0, k)$ we obtain quadratic limit points with respect to y of the x_1–system $\dot{x}_1 = \bar{f}(x_1, y, 0, k, 0)$ satisfying $\bar{g}(0, 0, 0, k, 0) = 0$. In the vicinity of these points the fast x_1–dynamics is given by

$$\begin{aligned} \dot{x}_1 \;&=\; \bar{f}(x_1, 0, 0, k, 0) \\ &=\; -\frac{1}{2 f_{2x_2}(0, k, 0)} \cdot \det\left(\begin{pmatrix} f_{1x_2} & f_{1x_1x_1} \\ f_{2x_2} & f_{2x_1x_1} \end{pmatrix} \right)(0, k, 0) \cdot x_1^2 \;+\; O(x_1^3) \end{aligned} \tag{4.5}$$

as can be seen by direct calculation. Recalling (3.8) the leading coefficient in (4.5) is well defined and different from zero for $k \neq 0$ which implies a saddle–node dynamics on the center manifold [14]. As expected the leading coefficient tends to infinity if we approach the Bogdanov point at $k = 0$. Since $\bar{g}(0, k, 0) = 0$ the points $(x_1, y, \lambda, k, \epsilon) = (0, 0, 0, k, 0)$ represent a curve of singularly perturbed saddle–nodes of the system (4.4) which implies a curve of singularly perturbed saddle–nodes $(x_1, x_2, y, \lambda, k, \epsilon) = (0, 0, 0, 0, k, 0)$ of the full system (3.7).

Singularly perturbed saddle–nodes have been examined in many papers; see for example [7], [10], [1], [9], [25]. It is well known that for fixed $k \neq 0$ a system of the form (4.4) typically gives rise to a (λ, ϵ)–unfolding diagram as shown in Fig.3.

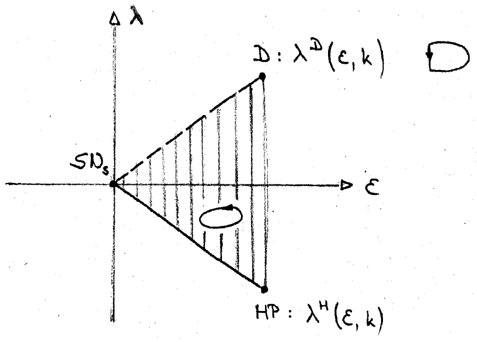

Figure 3: A typical (λ, ϵ)–unfolding diagram of a singularly perturbed saddle–node.

There exists a one–sided curve of Hopf points HP from which small periodic orbits bifurcate in the direction of λ as a consequence of coupling effects between the fast x–variable and the slow y–variable. The periodic orbits exist in the hatched region and they blow–up to some global object within an exponentially small strip of duck orbits indicated by the line D.

The precise location of $(\lambda^H, \lambda^D)(\epsilon, k)$ and the stability of the periodic orbits depend on certain derivatives of $\bar{f}$ and $\bar{g}$ at the singularly perturbed saddle–node. With the setting $(\bar{f}, \bar{g})^0 := (\bar{f}, \bar{g})(0, k, 0)$, $k \neq 0$ and with $-\bar{g}^0_{x_1} \bar{f}^0_y > 0$, the hatched region of periodic orbits exists for $\epsilon > 0$ and we obtain

$$\lambda^H_\epsilon(0, k) = -\frac{A + G}{B} \quad \text{and} \quad \lambda^D_\epsilon(0, k) = -\frac{(C + F)E + 3D}{BE^2} \tag{4.6}$$

where

$$\begin{aligned}
d &:= \sqrt{-\bar{g}^0_{x_1} \bar{f}^0_y} > 0, \\
A &:= \tfrac{1}{d^3} \cdot (\bar{f}_{x_1x_1}(\bar{f}_y \bar{g}_\epsilon - \bar{g}_y \bar{f}_\epsilon) - \bar{g}_{x_1}(\bar{f}_{\epsilon x_1} \bar{f}_y - \bar{f}_{yx_1} \bar{f}_\epsilon))^0, \\
B &:= \tfrac{1}{d^3} \cdot (\bar{f}_{x_1x_1}(\bar{f}_y \bar{g}_\lambda - \bar{g}_y \bar{f}_\lambda) - \bar{g}_{x_1}(\bar{f}_{\lambda x_1} \bar{f}_y - \bar{f}_{yx_1} \bar{f}_\lambda))^0 \neq 0, \\
C &:= \bar{f}^0_{x_1y}, \\
D &:= \tfrac{1}{6d} \cdot (\bar{f}_{x_1x_1x_1} \bar{f}^2_y - 3\bar{f}_{x_1y} \bar{f}_{x_1x_1} \bar{f}_y)^0, \\
E &:= \tfrac{1}{d} \cdot (\bar{f}_{x_1x_1} \bar{f}_y)^0 \neq 0, \\
F &:= \tfrac{1}{2d^2} \cdot (\bar{g}_{x_1x_1} \bar{f}^2_y - \bar{g}_y \bar{f}_{x_1x_1} \bar{f}_y)^0, \\
G &:= \tfrac{1}{d} \cdot \bar{g}^0_y
\end{aligned} \tag{4.7}$$

(cf. [24], [25] for details). The inequalities $\bar{g}^0_{x_1}$, $\bar{f}^0_y$, B, $E \neq 0$ follow by direct calculation from the conditions in (3.8). In case of $-\bar{g}^0_{x_1}\bar{f}^0_y < 0$ the periodic orbits exist for $\epsilon < 0$ and the formulas (4.6), (4.7) can be applied after performing the trivial transformation $\epsilon \to -\epsilon$.

Now the model equation (1.3) yields for $k > 0$ and $k < 0$ the left and right diagram in Fig.4 respectively.

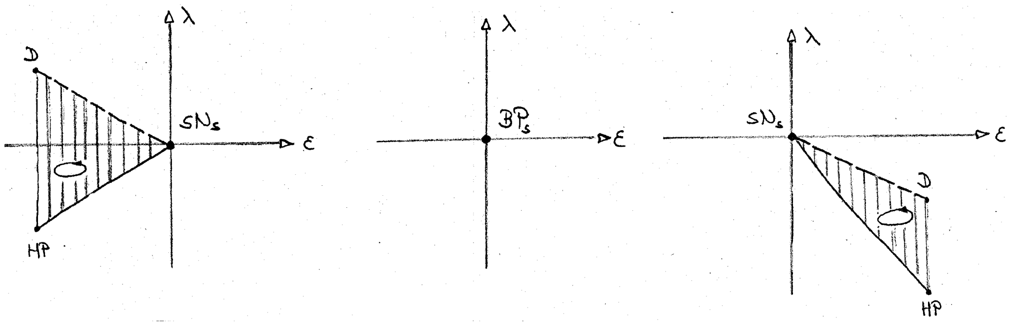

$k > 0$ $\qquad\qquad$ $k = 0$ $\qquad\qquad$ $k < 0$

Figure 4: The (λ,ϵ)–unfolding diagrams near the singularly perturbed saddle–nodes of the model equation (1.3).

For $k > (<)\ 0$ the periodic orbits exist locally for $\epsilon < (>)\ 0$. The derivative of the curve of Hopf points at $\epsilon = 0$ reads $\lambda^H_\epsilon(0,k) = \frac{1}{2k}$ whereas the duck orbits satisfy $\lambda^D_\epsilon(0,k) \equiv -\frac{1}{4}$. Note that our center manifold approach breaks down as k tends to zero and we obtain no information in the middle diagram at $k = 0$. The diagrams represent incomplete (λ,ϵ)–sections through the $(p_1,p_2,\epsilon) = (\lambda,k,\epsilon)$–unfolding diagram in Fig.2 near the singularly perturbed saddle–nodes SN_s. Similar results are valid for the general system (2.1) and hence for the FitzHugh–Nagumo equation (1.2) and the van der Pol–Duffing oscillator (2.8). The formulas become much more involved and we do not state them here. Note that the derivatives in (4.7) are calculated after the center manifold reduction is performed.

4.2 Unfolding singularly perturbed Hopf points

In this section we are looking for Hopf points of the x–system $\dot{x} = f(x,y,\lambda,k,0)$ from (3.7) which satisfy $g(x,y,\lambda,k,0) = 0$. The corresponding defining equation reads

$$\begin{pmatrix} f \\ \mathrm{tr}(f_x) \\ g \end{pmatrix}(x,y,\lambda,k,0) \;=:\; H(x,y,k,\lambda) \;=\; 0\;, \qquad H : \mathrm{I\!R}^5 \to \mathrm{I\!R}^4\;. \tag{4.8}$$

From (3.8) we obtain $H(0) = 0$ and $H_{x,y,k}(0)$ regular. Hence there exists a unique function $(x,y,k)^H(\lambda)$ with $(x,y,k)^H(0) = 0$ and $H[(x,y,k)^H(\lambda),\lambda] = 0$. Moreover with the setting $\bar{H}(\lambda) := \det(f_x)[(x,y)^H(\lambda),\lambda,k^H(\lambda),0]$ a simple calculation yields $\bar{H}'(0) = f^0_{2x_1x_1}g^0_\lambda/g^0_{x_1} \neq 0$; i.e. in case of $\bar{H}'(0) > (<)\ 0$ the curve $(x,y,k)^H(\lambda)$ represents for $\lambda > (<)\ 0$ a curve of Hopf points in the family of x–systems $\dot{x} = f(x,y,\lambda,k,0)$. Moreover we have $g = 0$ along this curve and hence a curve of singularly perturbed Hopf points occurs. The derivative of the k–component at $\lambda = 0$ reads

$$k^H_\lambda(0) \;=\; \frac{\mathrm{tr}_{x_1}(f_x)^0 \cdot g^0_\lambda \;-\; f^0_{2x_2\lambda}\cdot g^0_{x_1}}{f^0_{2x_2k}\cdot g^0_{x_1}}\;. \tag{4.9}$$

In case of $k_\lambda^H(0) \neq 0$ it is also possible to parametrize the singularly perturbed Hopf points by k. We obtain for $k_\lambda^H(0) \cdot \bar{H}'(0) > (<)\ 0$ and every fixed $k > (<)\ 0$ sufficiently small a singularly perturbed Hopf point HP_s (cf. diagram (a) in Fig.1 with $p_2 = k$) which can be unfolded with respect to λ and ϵ. Concerning the discussion of singularly perturbed Hopf points we restrict to the generic case $k_\lambda^H(0) \neq 0$. Hence the results are not applicable to the Hamiltonian case of the FitzHugh–Nagumo equation in a direct way (cf. diagram (b) in Fig.1). However, the unfolding diagrams of singularly perturbed saddle–nodes and homoclinic orbits are valid for the FitzHugh–Nagumo equation as well.

Now, a typical (λ, ϵ)–unfolding diagram of a singularly perturbed Hopf point is depicted in Fig.5. The proofs can be found in [24], [26].

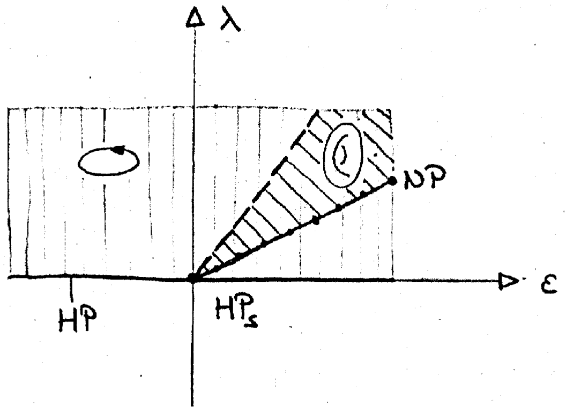

Figure 5: A typical (λ, ϵ)–unfolding diagram of a singularly perturbed Hopf point.

There exists a curve of Hopf points HP through the central point HP_s (transversal to the λ–axis) from which periodic orbits bifurcate in the direction of λ. The periodic orbits exist in the weakly hatched region which represents a 2–dimensional surface of periodic orbits. This surface contains a curve NP of periodic orbits with a conjugate–complex pair of Floquet multipliers on the unit circle. Typically these orbits give rise to invariant tori [14] that are indicated in the cross hatched region. The precise properties of this region are not known and its border is indicated by a broken line and drawn in an arbitrary fashion.

However, note that at $\epsilon = 0$ not any invariant torus can survive in the resulting 2–dimensional system $\dot{x} = f$, $\dot{y} = 0$. This is a typical feature of singular perturbation problems, where the lower dimensional $\epsilon = 0$ system cannot show the higher dimensional phenomena that may exist in the full system. Note also that the invariant tori appear as a consequence of coupling effects between the fast x–variables and the slow y–variable.

The precise location of the curves HP, NP and the specific features of the periodic orbits (bifurcation direction, stability, ...) depend on certain derivatives of f and g in the singularly perturbed Hopf point (cf. [24], [26] for details). However, it is rather cumbersome to calculate explicitly in a concrete example (even in case of the model equation (1.3)) all the characteristic coefficients that determine quantitatively the unfolding structure. Higher order variational equations must be solved at the singularly perturbed Hopf point which suggests using computeralgebraic programs. In the following we mainly restrict to numerical results.

In case of the model equation (1.3) we obtain for fixed $k > 0$ the (λ, ϵ)–unfolding diagram shown in diagram (a) of Fig.6. The singularly perturbed Hopf point HP_s and the Naimark–

Sacker points NP are positioned at $(\lambda, \epsilon) = (-k, 0)$ and $(\lambda, \epsilon) = (-k, \epsilon)$, $\epsilon > 0$ respectively. The Hopf points HP are given by $\epsilon = 2\lambda(\lambda + k)$, $\lambda < 0$.

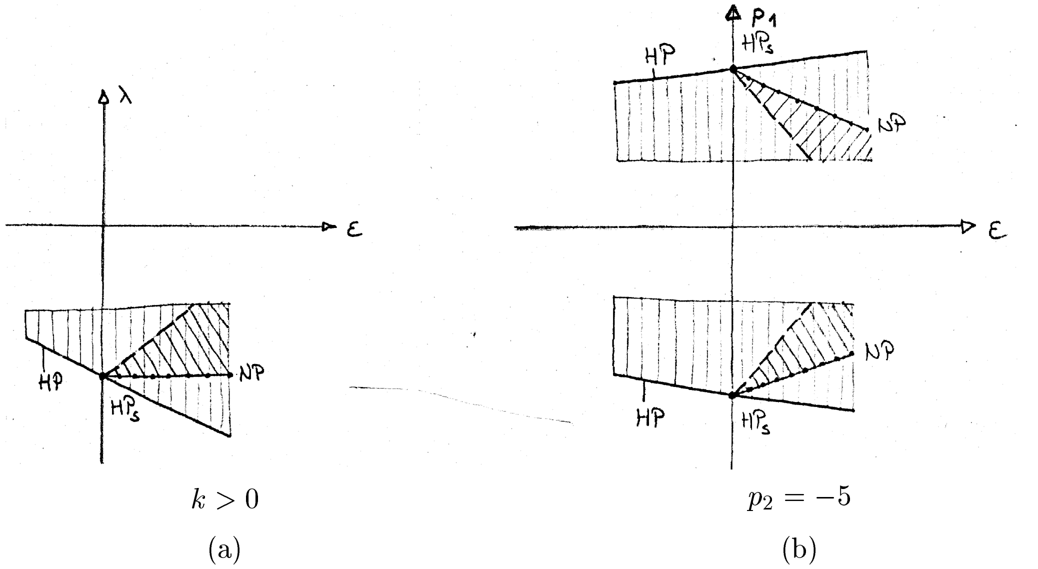

Figure 6: The (λ, ϵ)–unfolding diagrams near the singularly perturbed Hopf points of the model equation (a) and the van der Pol–Duffing oscillator (b).

In case of the van der Pol–Duffing oscillator the singularly perturbed Hopf points occur at $p_1 = \pm(p_2 + \frac{8}{3})/\sqrt{3}$, $p_2 < -4$ and we obtain at $p_2 = -5$ the (p_1, ϵ)–unfolding diagram (b) in Fig.6. A diagram of this type (with other parameter values) can be found in [18] Fig.12(a).

Remember that Fig.4 and diagram (a) in Fig.6 show the local (λ, ϵ)–unfoldings of the model equation (1.3) near the singularly perturbed saddle–node and Hopf points. These local diagrams are connected by the parabolic Hopf curve $\epsilon = 2\lambda(\lambda + k)$, $\lambda < 0$ and we obtain for fixed $k > 0$ the (λ, ϵ)–diagram as indicated in Fig.7. Moreover, the dotted NP–points terminate at the point NP_{-1} that represents a periodic orbit with double Floquet multiplier -1. Hence the two Floquet multipliers different from zero are moving along the unit circle from 1 to -1 during variation along the curve of NP–points (cf. diagram (b) in Fig.2).

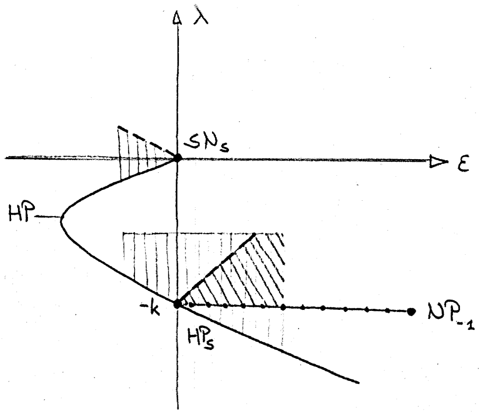

Figure 7: The (λ, ϵ)–section through Fig.2 near the points SN_s and HP_s for fixed $k > 0$.

Fig.7 shows a detailed (λ, ϵ)–section through the (λ, k, ϵ)–unfolding diagram in Fig.2 for fixed $k > 0$. The homoclinic orbits Ho are not taken into consideration in Fig.7. This will be done in the next section.

5 Homoclinic orbits obtained by a blow–up transformation

In Fig.8 we redraw in detail the numerically calculated surface of homoclinic orbits Ho of the model equation (1.3) from Fig.2.

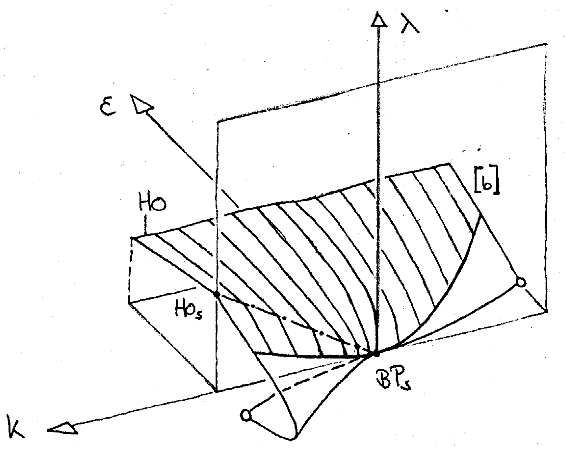

Figure 8: The surface of homoclinic orbits for the model equation.

For graphical reasons we changed the direction of the ϵ–axis. Our aim is to verify analytically the hatched upper part of the surface which includes the singularly perturbed homoclinic orbits Ho_s in the $(p_1, p_2) = (\lambda, k)$–plane. This is done for the general system (3.7) which was derived from system (2.1) under the assumptions (2.2)–(2.4). In addition we investigate more closely by numerical calculations the lower part of the surface; i.e. we investigate the approach to the border line of open circles where a duck like behavior of the homoclinic orbits seems to occur.

5.1 Analytical results

The analytical results are obtained with a theorem from [3] which can be applied after the singularly perturbed Bogdanov point $(x, y, \lambda, k, \epsilon) = 0$ is blown–up appropriately. This scaling transformation between the old variables $(x_1, x_2, y, \epsilon, \lambda, k, t)$ and the new variables $(u_1, u_2, v, \bar{\epsilon}, \bar{\lambda}, \bar{k}, \tau)$ reads

$$\begin{array}{llcl} \text{coordinates :} & (x_1\ ,\ x_2\ ,\ y) & = & (c_1 \cdot \bar{\lambda}^2 \cdot u_1\ ,\ c_2 \cdot \bar{\lambda}^3 \cdot u_2\ ,\ c_3 \cdot \bar{\lambda}^4 \cdot v) \\ \text{parameters :} & (\epsilon\ ,\ \lambda\ ,\ k) & = & (c_4 \cdot \bar{\lambda}^3 \cdot \bar{\epsilon}\ ,\ c_5 \cdot \bar{\lambda}^2\ ,\ c_6 \cdot \bar{\lambda}^2 \cdot \bar{k}) \\ \text{time :} & t & = & c_7 \cdot \bar{\lambda}^{-1} \cdot \tau \end{array} \tag{5.1}$$

where we used u and v again to denote the new coordinates. The constants $c_1, ..., c_7$ will be chosen later on. Essentially this $\bar{\lambda}$–scaling is a direct extension of the well known scaling near a regularly perturbed Bogdanov point [14]. However, note that we maintain a linear dependence between the variables y and v. This seems appropriate because v represents a dynamic variable for $\bar{\epsilon} \neq 0$ and it is convenient to decouple the parameter transformation between (ϵ, λ, k) and $(\bar{\epsilon}, \bar{\lambda}, \bar{k})$ from the coordinate transformation between (x_1, x_2, y) and (u_1, u_2, v). Then a straightforward calculation yields the transformed system

$$\begin{aligned} \dot{u}_1 &= u_2 + \bar{\lambda} \cdot (a_1 u_1^2 + a_2 v) + O(\bar{\lambda}^2) \\ &=: F_1(u_1, u_2, v, \bar{\lambda}, \bar{k}, \bar{\epsilon}) \\ \dot{u}_2 &= u_1^2 - v + \bar{\lambda} \cdot (b_1 u_1 u_2 + b_2 \bar{k} u_2 + b_3 u_2) + O(\bar{\lambda}^2) \\ &=: F_2(u_1, u_2, v, \bar{\lambda}, \bar{k}, \bar{\epsilon}) \\ \dot{v} &= \bar{\epsilon} \cdot [\, u_1 - 2 + O(\bar{\lambda}) \,] \\ &=: \bar{\epsilon} \cdot G(u_1, u_2, v, \bar{\lambda}, \bar{k}, \bar{\epsilon}) \end{aligned} \tag{5.2}$$

which maintains the singular perturbation form. The constants in (5.1) are chosen according to

$$\begin{array}{llll} \text{coordinates :} & c_1 = \frac{1}{2} f^0_{2x_1x_1} , & c_2 = c_1^2 , & c_3 = -c_1^3 / f^0_{2y} \\ \text{parameters :} & c_4 = -c_1^3 / (f^0_{2y} \cdot g^0_{x_1}) , & c_5 = -2\, c_1\, g^0_{x_1} / g^0_\lambda , & c_6 = c_1 \\ \text{time :} & c_7 = 1/c_1 . & & \end{array} \tag{5.3}$$

This yields the following coefficients for the linear $\bar{\lambda}$–terms in (5.2)

$$\begin{array}{lll} a_1 = \frac{1}{2} f^0_{1x_1x_1} , & a_2 = -\frac{1}{2} f^0_{2x_1x_1} \cdot f^0_{1y} / f^0_{2y} , & \\ b_1 = f^0_{2x_1x_2} , & b_2 = f^0_{2x_2k} , & b_3 = -2\, f^0_{2x_2\lambda} \cdot g^0_{x_1} / g^0_\lambda . \end{array} \tag{5.4}$$

According to (3.3) and (3.8), (3.10) these coefficients are completely expressed in terms of derivatives of the original system (2.1) evaluated at the singularly perturbed Bogdanov point. Under the assumptions (2.2)–(2.4) and (3.1) the coefficients may assume arbitrary values. In the next step we shall impose conditions on the coefficients which ensure the existence of homoclinic orbits of the system (5.2) for $\bar{\epsilon} \neq 0$. In particular the difference between the assumption (3.1) and the stronger assumption (2.7) of a generic unfolding is analyzed.

First we are looking for homoclinic orbits of the fast u–system $\dot{u} = F$ at $\bar{\epsilon} = 0$. Secondly we identify among these orbits the homoclinic orbits whose base points satisfy $G = 0$ and thirdly we continue these singularly perturbed homoclinic orbits to $\bar{\epsilon} \neq 0$ with the help of an appropriate Melnikov condition.

Homoclinic orbits at $\bar{\epsilon} = 0$

At $\bar{\epsilon} = 0$, $\bar{\lambda} = 0$ and $\bar{k} \in \mathbb{R}$ the fast u–system $\dot{u}_1 = u_2$, $\dot{u}_2 = u_1^2 - v$ in (5.2) represents a well known v–dependent family of Hamiltonian systems [14] with corresponding family of homoclinic orbits

$$\begin{aligned} \bar{u}_1(\tau, v) &= v^{\frac{1}{2}} \cdot [\, 1 - 3 \operatorname{sech}^2 \left(2^{-\frac{1}{2}}\, v^{\frac{1}{4}}\, \tau \right) \,] \\ \bar{u}_2(\tau, v) &= 3\sqrt{2}\, v^{\frac{3}{4}} \cdot \operatorname{sech}^2 \left(2^{-\frac{1}{2}}\, v^{\frac{1}{4}}\, \tau \right) \cdot \tanh \left(2^{-\frac{1}{2}}\, v^{\frac{1}{4}}\, \tau \right) \end{aligned} \tag{5.5}$$

for $v > 0$. Note that the base points $\bar{u}(\infty, v)$ of the homoclinic orbits are

$$\bar{u}_1(\infty, v) \;=\; \sqrt{v}\;, \qquad \bar{u}_2(\infty, v) \;=\; 0\;, \qquad v \;>\; 0\;. \tag{5.6}$$

Hence in the 3–dimensional $(v, \bar{\lambda}, \bar{k})$–parameter space of the u–system $\dot{u} = F(u, v, \lambda, \bar{k}, 0)$ we obtain a surface of homoclinic orbits at $\bar{\lambda} = 0$ as indicated in diagram (a) of Fig.9. Obviously this trivial surface exists for arbitrary values of the coefficient b_2.

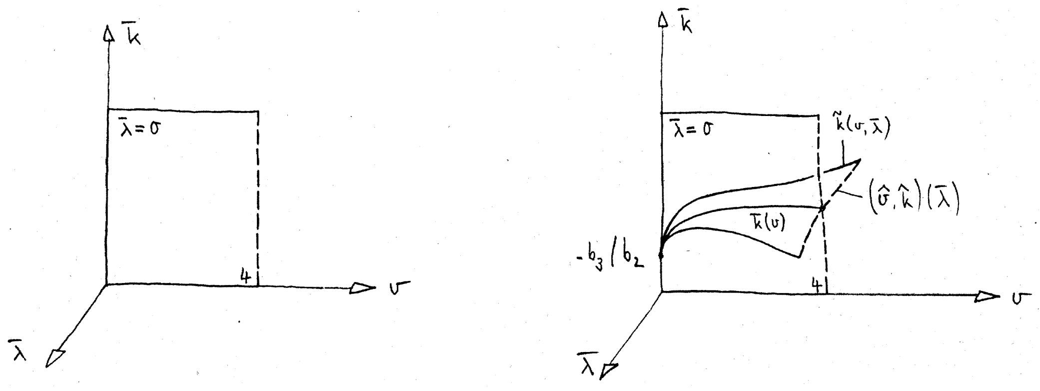

$b_2 \in \mathbb{R}$ $\qquad$ $b_2 \neq 0$

(a) $\qquad$ (b)

Figure 9: The system (5.2) at $\bar{\epsilon} = 0$: (a) The trivial surface of homoclinic orbits obtained by the blow–up, (b) The nontrivial surface of homoclinic orbits in case of a generic unfolding.

Next we continue some of these homoclinic orbits to $\bar{\lambda} \neq 0$. This leads to diagram (b) in Fig.9 under the additional restriction $b_2 = f^0_{2x_2k} \neq 0$ which is satisfied for a generic unfolding of a singularly perturbed Bogdanov point (cf. (3.10)). Without the extra v–parameter, bifurcation results of this type are derived in [6], [14] and [2], so we restrict to the special features of our situation.

First the bifurcation condition which is equivalent to a vanishing Melnikov function with respect to $\bar{\lambda}$ reads

$$\begin{aligned}
0 \;&=\; -\int_{-\infty}^{\infty} [-\dot{\bar{u}}_2,\ \dot{\bar{u}}_1] \cdot F_{\bar{\lambda}}(\bar{u}, v, 0, \bar{k}, 0)\ d\tau \\
&=\; -\int_{-\infty}^{\infty} -\ddot{\bar{u}}_1 \cdot (a_1\bar{u}_1^2 \;+\; a_2 v) \;+\; \dot{\bar{u}}_1^2 \cdot (b_1\bar{u}_1 \;+\; b_2\bar{k} \;+\; b_3)\ d\tau \\
&=\; -(2a_1 \;+\; b_1) \cdot \int_{-\infty}^{\infty} \dot{\bar{u}}_1^2 \bar{u}_1\ d\tau \;-\; (b_2\bar{k} \;+\; b_3) \cdot \int_{-\infty}^{\infty} \dot{\bar{u}}_1^2\ d\tau \\
&=\; \sqrt{2}\,\tfrac{24}{35}\, v^{\frac{5}{4}} \cdot [\ 5(2a_1 \;+\; b_1)\,\sqrt{v} \;-\; 7(b_2\bar{k} \;+\; b_3)\ ] \;=:\; M(v, \bar{k})\;.
\end{aligned} \tag{5.7}$$

In case of $b_2 \neq 0$ we obtain $M(v, \bar{k}) = 0$, $v > 0$ iff

$$\bar{k} \;=\; \frac{5(2a_1 \;+\; b_1)\,\sqrt{v} \;-\; 7b_3}{7b_2} \;=:\; \bar{k}(v)\;. \tag{5.8}$$

Finally the nondegeneracy condition for bifurcations along $\bar{k}(v)$ reads

$$0 \neq \int_{-\infty}^{\infty} [-\dot{\bar{u}}_2,\ \dot{\bar{u}}_1] \cdot F_{\bar{\lambda}\bar{k}}(\bar{u}, v, 0, \bar{k}(v), 0)\ d\tau = b_2 \cdot \int_{-\infty}^{\infty} \dot{\bar{u}}_1^2\ d\tau \tag{5.9}$$

which is true according to $b_2 \neq 0$. Hence we obtain a nontrivial surface of homoclinic orbits

$$[\ u, v, \bar{\lambda}, \bar{k}\ ] = [\ \tilde{u}(\tau, v, \bar{\lambda}),\ v,\ \bar{\lambda},\ \tilde{k}(v, \bar{\lambda})\ ], \qquad v > 0, \qquad |\bar{\lambda}| \ll 1 \tag{5.10}$$

with $\tilde{u}(\tau, v, 0) = \bar{u}(\tau, v)$ and $\tilde{k}(v, 0) = \bar{k}(v)$ (cf. diagram (b) in Fig.9). Summarizing, the fast u–system $\dot{u} = F(u, v, \bar{\lambda}, \bar{k}, 0)$ has the trivial surface (5.5) of homoclinic orbits at $\bar{\lambda} = 0$ which is intersected at $(v, \bar{\lambda}, \bar{k}) = (v, 0, \bar{k}(v))$ by the nontrivial surface (5.10) in case of $b_2 \neq 0$.

Up to now we performed a well known bifurcation analysis of homoclinic orbits. In the next section we extend this bifurcation analysis to the full (x, y)–system (5.2) with respect to the singular perturbation parameter $\bar{\epsilon}$; i.e. we determine in Fig.9 the homoclinic orbits that can be continued to $\bar{\epsilon} \neq 0$.

As already mentioned a generic unfolding of a singularly perturbed Bogdanov point implies $b_2 = f^0_{2x_2k} \neq 0$ and diagram (b) in Fig.9 occurs. However, our approach allows to treat the degenerate case $b_2 = 0$ almost without extra effort, so we include this case.

The bifurcation analysis with respect to $\bar{\epsilon}$

Our aim is to apply the bifurcation result from [3] which can be stated as follows. Consider a singularly perturbed system of the form

$$\begin{aligned} \dot{u} &= F(u, v, \lambda, \epsilon) \in \mathbb{R}^n, \qquad n \geq 2 \\ \dot{v} &= \epsilon \cdot G(u, v, \lambda, \epsilon) \in \mathbb{R} \end{aligned} \tag{5.11}$$

and assume the steady state conditions

$$\begin{gathered} (F, G)^0 := (F, G)(0, 0, 0, 0) = 0, \qquad F^0_u \quad \text{hyperbolic}, \\ \begin{pmatrix} F_u & F_v \\ G_u & G_v \end{pmatrix}^0 \quad \text{nonsingular}\ . \end{gathered} \tag{5.12}$$

This implies the existence of a unique function $(u, v)^s(\lambda, \epsilon)$ such that

$$\begin{gathered} (F, G)((u, v)^s(\lambda, \epsilon), \lambda, \epsilon) = 0, \qquad (u, v)^s(0, 0) = 0, \\ \begin{pmatrix} u^s_\lambda & u^s_\epsilon \\ v^s_\lambda & v^s_\epsilon \end{pmatrix}(0, 0) = -\begin{pmatrix} F^0_u & F^0_v \\ G^0_u & G^0_v \end{pmatrix}^{-1} \cdot \begin{pmatrix} F^0_\lambda & F^0_\epsilon \\ G^0_\lambda & G^0_\epsilon \end{pmatrix}. \end{gathered} \tag{5.13}$$

Further, concerning the dynamical properties we assume that the system $\dot{u} = F(u, 0, 0, 0)$ has a homoclinic orbit $\bar{u}(\tau)$ with base point $u = 0$ such that the only bounded solutions of the homogenous equation

$$\dot{u} = F_u(\bar{u}(\tau), 0, 0, 0) \cdot u \qquad \text{are} \qquad u = c\dot{\bar{u}}, \quad c \in \mathbb{R}\ . \tag{5.14}$$

This condition represents an internal regularity condition of the central homoclinic orbit. Moreover we assume the external regularity condition with respect to λ

$$M \;:=\; -\int_{-\infty}^{\infty} \Psi^T(\tau)\cdot[F_u,F_v,F_\lambda](\bar u(\tau),0,0,0)\cdot\begin{pmatrix} u^s_\lambda(0,0)\\ v^s_\lambda(0,0)\\ 1\end{pmatrix} d\tau \;\neq\; 0 \tag{5.15}$$

which can be interpreted as a transversality or Melnikov condition along the branch $(u,v)^s(\lambda,0)$. Here $\Psi(\tau)$ denotes the unique bounded solution (up to a constant multiple) of the adjoint equation $\dot u = -F_u^T(\bar u(\tau),0,0,0)u$ (cf. [22]).

Note that the equations (5.11)–(5.15) are dealing with a homoclinic base point of the u–system $\dot u = F(u,v,0,0)$ which satisfies $G=0$; i.e. we treat a singularly perturbed homoclinic base point. This point is assumed to lie in the origin without loss of generality.

Finally assume for definiteness $(G_u\cdot F_u^{-1}\cdot F_v - G_v)^0 < 0$ which can always be achieved by time reversal. Then we obtained in [3] the following bifurcation result. There exist $\epsilon_0>0$ and differentiable functions

$$\begin{aligned} \lambda^+(\epsilon) &= \lambda_1^+\cdot\epsilon + O(\epsilon^2), && 0\le\epsilon\le\epsilon_0\\ \lambda^-(\epsilon) &= \lambda_1^-\cdot\epsilon + O(\epsilon^2), && -\epsilon_0\le\epsilon\le 0 \end{aligned} \tag{5.16}$$

such that the system (5.11) has homoclinic orbits $(u^\pm,v^\pm)(\tau,\epsilon)$ at $(\lambda,\epsilon)=(\lambda^\pm(\epsilon),\epsilon)$ with $(u^\pm,v^\pm)(\tau,0)=(\bar u(\tau),0)$ and $\lambda^\pm(0)=0$. The right and left derivative λ_1^+ and λ_1^- can be expressed as

$$\begin{aligned} \lambda_1^+ = \frac{1}{M}\cdot\int_{-\infty}^{\infty}\Psi^T(\tau)\cdot\Bigg\{ & -[F_u,F_v](\bar u(\tau),0,0,0)\cdot\begin{pmatrix} -(F_u^{-1}F_v)^0\\ 1\end{pmatrix}\cdot\int_\tau^\infty G(\bar u(s),0,0,0)ds\\ & + [F_u,F_v,F_\epsilon](\bar u(\tau),0,0,0)\cdot\begin{pmatrix} u^s_\epsilon(0,0)\\ v^s_\epsilon(0,0)\\ 1\end{pmatrix} + (F_u^{-1}F_v)^0\cdot G(\bar u(\tau),0,0,0)\Bigg\}\, d\tau \end{aligned} \tag{5.17}$$

and

$$\begin{aligned} \lambda_1^- = \frac{1}{M}\cdot\int_{-\infty}^{\infty}\Psi^T(\tau)\cdot\Bigg\{ & [F_u,F_v](\bar u(\tau),0,0,0)\cdot\begin{pmatrix} -(F_u^{-1}F_v)^0\\ 1\end{pmatrix}\cdot\int_{-\infty}^\tau G(\bar u(s),0,0,0)ds\\ & + [F_u,F_v,F_\epsilon](\bar u(\tau),0,0,0)\cdot\begin{pmatrix} u^s_\epsilon(0,0)\\ v^s_\epsilon(0,0)\\ 1\end{pmatrix} + (F_u^{-1}F_v)^0\cdot G(\bar u(\tau),0,0,0)\Bigg\}\, d\tau \end{aligned} \tag{5.18}$$

(for u^s_ϵ, v^s_ϵ see (5.13)). Hence we obtain two nontrivial curves of homoclinic orbits for $\epsilon>0$ ($\epsilon<0$) both of which emanate from $(\lambda,\epsilon)=0$. Generically, these curves meet transversally at $\epsilon=0$ due to $\lambda_1^+\neq\lambda_1^-$. Similar results appear in [27], [17] where general transversality arguments are used to prove the pure existence of homoclinic orbits for $\epsilon\neq 0$. The precise quantitative behavior of the homoclinic solutions, for example the ϵ–expansions or the asymptotic time estimates of $(u^\pm,v^\pm)(\tau,\epsilon)$ can be found in [3].

We apply the above results to the blown–up system (5.2). This is done twice with respect to $(\lambda, \epsilon) = (\bar{\lambda}, \bar{\epsilon})$ and $(\lambda, \epsilon) = (\bar{k}, \bar{\epsilon})$ respectively. In the last section we determined the homoclinic orbits at $\bar{\epsilon} = 0$. Next we identify the homoclinic orbits whose base points satisfy $G(u, v, \bar{\lambda}, \bar{k}, 0) = 0$ in addition. This simple condition represents the bifurcation equation.

Recalling that $(u_1, u_2, v, \bar{\lambda}, \bar{k}) = (\sqrt{v}, 0, v, 0, \bar{k})$ are homoclinic base points of the trivial surface (cf. (5.6)) we obtain

$$G[\ \sqrt{v},\ 0,\ v,\ 0,\ \bar{k},\ 0\ ] \ = \ \sqrt{v} - 2 \ = \ 0 \qquad \text{iff} \qquad v = 4, \qquad \bar{k} \in \mathbb{R}\ . \tag{5.19}$$

This leads to the vertical broken line in the diagrams of Fig.9 at $v = 4$, $\bar{\lambda} = 0$. Concerning the nontrivial homoclinic orbits in case of $b_2 \neq 0$ we consider (cf. (5.10))

$$\begin{aligned} G[\ \tilde{u}(\infty, v, \bar{\lambda}),\ v,\ \bar{\lambda},\ \tilde{k}(v, \bar{\lambda}),\ 0\ ] \ &= \ \tilde{u}_1(\infty, v, 0) \ - \ 2 \ + \ O(\bar{\lambda}) \\ &= \ \sqrt{v} \ - \ 2 \ + \ O(\bar{\lambda}) \ = \ 0 \end{aligned} \tag{5.20}$$

and obtain a locally unique function $\hat{v}(\bar{\lambda})$ with $\hat{v}(0) = 4$ satisfying

$$G[\ \tilde{u}(\infty, \hat{v}(\bar{\lambda}), \bar{\lambda}),\ \hat{v}(\bar{\lambda}),\ \bar{\lambda},\ \tilde{k}(\hat{v}(\bar{\lambda}), \bar{\lambda}),\ 0\ ] \ = \ 0\ . \tag{5.21}$$

We define $(\hat{u}, \hat{k})(\bar{\lambda}) := [\tilde{u}(\infty, \hat{v}(\bar{\lambda}), \bar{\lambda}), \tilde{k}(\hat{v}(\bar{\lambda}), \bar{\lambda})]$ and denote the corresponding homoclinic orbits by $\hat{u}(\tau, \bar{\lambda})$.

Summarizing, broken lines in Fig.9 indicate the homoclinic orbits at $\bar{\epsilon} = 0$ which satisfy the bifurcation equation $G = 0$ and it remains to verify the nondegeneracy conditions in (5.12), (5.14) and (5.15) for proving bifurcation with respect to $\bar{\epsilon}$.

First we obtain from (5.2) the regularity of the matrix

$$\begin{pmatrix} F_u & F_v \\ G_u & G_v \end{pmatrix} (\sqrt{v}, 0, v, 0, \bar{k}, 0) \ = \ \begin{pmatrix} 0 & 1 & 0 \\ 2\sqrt{v} & 0 & -1 \\ 1 & 0 & 0 \end{pmatrix}$$

as desired (cf. (5.12)). Thus we have a unique surface of steady states $(u, v)^s(\bar{\lambda}, \bar{k}, \bar{\epsilon})$ with

$$\begin{aligned} &(F, G)[\ (u, v)^s(\bar{\lambda}, \bar{k}, \bar{\epsilon})\ , \bar{\lambda},\ \bar{k},\ \bar{\epsilon}\ ] \ = \ 0 \qquad \text{and} \\ &(u, v)^s(0, \bar{k}, 0) \ \equiv \ (2, 0, 4), \qquad (u, v)^s(\bar{\lambda}, \hat{k}(\bar{\lambda}), 0) \ = \ (\hat{u}, \hat{v})(\bar{\lambda}) \end{aligned} \tag{5.22}$$

(cf. (5.13)). Secondly, the condition (5.14) is satisfied along the broken lines in Fig.9 at $\bar{\lambda} = 0$ as can be seen from the behavior of the Wronski–determinant of the system $\dot{u} = F_u(\bar{u}(\tau, 4), 4, 0, \bar{k}, 0)u$ as τ tends to infinity. Concerning the nontrivial homoclinic orbits in Fig.9 this property follows locally from a perturbation argument.

Finally, we verify the Melnikov condition (5.15) separately along $[u, v, \bar{\lambda}, \bar{k}, \bar{\epsilon}] = [\bar{u}(\tau, 4), 4, 0, \bar{k}, 0]$ with respect to $(\lambda, \epsilon) = (\bar{\lambda}, \bar{\epsilon})$ and along $[u, v, \bar{\lambda}, \bar{k}, \bar{\epsilon}] = [\hat{u}(\tau, \bar{\lambda}), \hat{v}(\bar{\lambda}), \bar{\lambda}, \hat{k}(\bar{\lambda}), 0]$ with respect to $(\lambda, \epsilon) = (\bar{k}, \bar{\epsilon})$.

First we continue the homoclinic orbits $[u, v, \bar{\lambda}, \bar{k}, \bar{\epsilon}] = [\bar{u}(\tau, 4), 4, 0, \bar{k}, 0]$ in the $(\bar{\lambda}, \bar{\epsilon})$–plane. In this case the Melnikov condition reads

$$
\begin{aligned}
0 \;&\neq\; - \int_{-\infty}^{\infty} [-\dot{\bar{u}}_2,\ \dot{\bar{u}}_1](\tau, 4) \cdot [F_u, F_v, F_{\bar{\lambda}}](\bar{u}(\tau, 4), 4, 0, \bar{k}, 0) \cdot \begin{pmatrix} u^s_{\bar{\lambda}}(0, \bar{k}, 0) \\ v^s_{\bar{\lambda}}(0, \bar{k}, 0) \\ 1 \end{pmatrix} d\tau \\
&=\; - \int_{-\infty}^{\infty} [-\dot{\bar{u}}_2,\ \dot{\bar{u}}_1](\tau, 4) \cdot F_{\bar{\lambda}}(\bar{u}(\tau, 4), 4, 0, \bar{k}, 0)\ d\tau \;=\; M(4, \bar{k})
\end{aligned}
\tag{5.23}
$$

(cf. (5.7)). Note that $\int_{-\infty}^{\infty} \dot{\bar{u}}_1\ d\tau = \int_{-\infty}^{\infty} \dot{\bar{u}}_2\ d\tau = \int_{-\infty}^{\infty} \dot{\bar{u}}_1 \bar{u}_1\ d\tau = 0$. According to (5.7), (5.8) this nondegeneracy condition is satisfied for

$$
\bar{k} \in \mathbb{R} \qquad \text{in case of} \qquad b_2 \;=\; 0, \qquad 10(2a_1 \;+\; b_1) \;-\; 7b_3 \;=:\; \gamma \;\neq\; 0 \tag{5.24}
$$

and for

$$
\bar{k} \;\neq\; \bar{k}(4) \;=\; \frac{\gamma}{7b_2} \qquad \text{in case of} \qquad b_2 \;\neq\; 0\ . \tag{5.25}
$$

Thus, in the $(\bar{\lambda}, \bar{k}, \bar{\epsilon})$–parameter space of the system (5.2) we obtain smooth $\bar{k}$–dependent surfaces (cf. (5.16))

$$
\bar{\lambda} \;=\; \bar{\lambda}^{+}(\bar{k}, \bar{\epsilon}), \quad 0 \leq \bar{\epsilon} \leq \bar{\epsilon}_0(\bar{k}) \qquad \text{and} \qquad \bar{\lambda} \;=\; \bar{\lambda}^{-}(\bar{k}, \bar{\epsilon}), \quad -\bar{\epsilon}_0(\bar{k}) \leq \bar{\epsilon} \leq 0 \tag{5.26}
$$

of homoclinic orbits which branch off from the $\bar{k}$–axis for $\bar{k} \in \mathbb{R}$ in case of $b_2 = 0$, $\gamma \neq 0$ (cf. diagram (a) in Fig.10) and for $\bar{k} \in \mathbb{R} \setminus \{\bar{k}(4)\}$ in case of $b_2 \neq 0$ (cf. diagram (b) in Fig.10). However, note that the proof in [3] does not describe in detail the limiting behaviour of $\bar{\epsilon}_0(\bar{k})$ as $\bar{k}$ tends to $\pm\infty$ or as $\bar{k}$ tends to $\bar{k}(4)$ in case of $b_2 \neq 0$. We only know $\bar{\epsilon}_0(\bar{k}) \to 0$ in these situations.

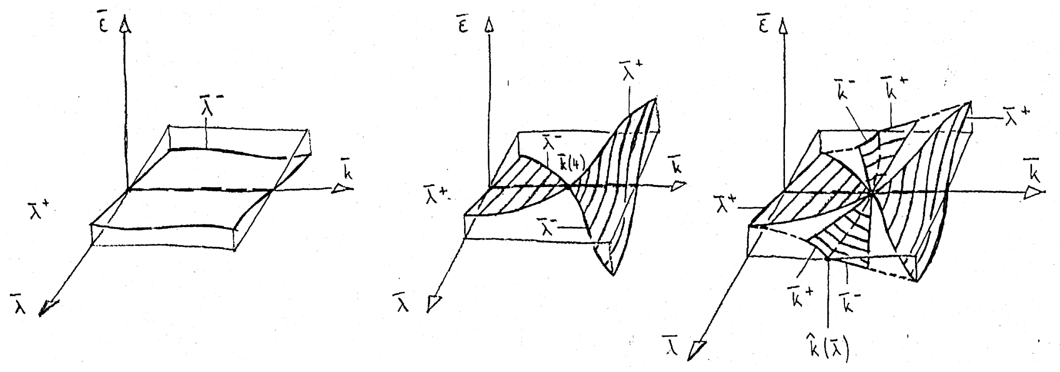

(a) (b) (c)

Figure 10: The surfaces of homoclinic orbits of the blown–up system (5.2) : (a) $b_2 = 0$, $\gamma \neq 0$, (b) and (c) $b_2 \neq 0$.

Further it is not difficult to see the antisymmetry $\bar{\lambda}^{+}(\bar{k}, \bar{\epsilon}) = -\bar{\lambda}^{-}(\bar{k}, -\bar{\epsilon})$ which results from a certain symmetry of the scaling transformation (5.1) and a uniqueness argument (cf. [2]). In particular the surfaces are smooth along the $\bar{k}$–axis, i.e. the derivatives at $\bar{\epsilon} = 0$ satisfy $\bar{\lambda}_1^{-}(\bar{k}) = \bar{\lambda}_1^{+}(\bar{k})$ (cf. (5.16)) and the homoclinic orbits which correspond to $\bar{\lambda} = \bar{\lambda}^{+}(\bar{k}, \bar{\epsilon})$ and

$\bar{\lambda} = -\bar{\lambda}^-(\bar{k}, -\bar{\epsilon})$ are representing the same homoclinic orbit of the unscaled system (3.7). Hence we can restrict to

$$\bar{\lambda}^+(\bar{k}, \bar{\epsilon}) \;=\; \bar{\lambda}_1^+(\bar{k}) \cdot \bar{\epsilon} \;+\; O(\bar{\epsilon}^2), \quad 0 \le \bar{\epsilon} \le \bar{\epsilon}_0(\bar{k}) \; . \tag{5.27}$$

The derivative $\bar{\lambda}_1^+(\bar{k})$ at $\bar{\epsilon} = 0$ follows after some calculations from (5.17) according to

$$\bar{\lambda}_1^+(\bar{k}) \;=\; \frac{1}{M(4,\bar{k})} \cdot \int_{-\infty}^{\infty} [\; \bar{u}_1(\tau, 4) - 2 \;]^2 \; d\tau \;=\; \frac{35}{4} \cdot \frac{1}{\gamma - 7 b_2 \bar{k}} \; . \tag{5.28}$$

In case of $b_2 \neq 0$ this derivative has a pole at $\bar{k} = \bar{k}(4)$ and converges to zero as $\bar{k} \to \pm\infty$. In case of $b_2 = 0$ we obtain the identity $\bar{\lambda}_1^+(\bar{k}) \equiv 35/(4\gamma)$.

It remains to verify in case of $b_2 \neq 0$ the Melnikov condition (5.15) along the homoclinic orbits $[u, v, \bar{\lambda}, \bar{k}, \bar{\epsilon}] = [\hat{u}(\tau, \bar{\lambda}), \hat{v}(\bar{\lambda}), \bar{\lambda}, \hat{k}(\bar{\lambda}), 0]$ with respect to $(\bar{k}, \bar{\epsilon})$. Let $\psi(\tau, \bar{\lambda})$ denote the unique bounded solution (up to a scalar multiple) of the corresponding adjoint equation $\dot{u} = -F_u^T[\hat{u}(\tau, \bar{\lambda}), \hat{v}(\bar{\lambda}), \bar{\lambda}, \hat{k}(\bar{\lambda}), 0]u$. $\psi(\tau, \bar{\lambda})$ can be chosen to vary smoothly in $(\tau, \bar{\lambda})$ and to satisfy $\psi^T(\tau, 0) = [-\dot{\bar{u}}_2, \dot{\bar{u}}_1](\tau, 4)$. Then the nondegeneracy condition reads

$$\begin{aligned} 0 \;&\neq\; -\int_{-\infty}^{\infty} \psi^T(\tau, \bar{\lambda}) \cdot [F_u, F_v, F_{\bar{k}}][\hat{u}(\tau, \bar{\lambda}), \hat{v}(\bar{\lambda}), \bar{\lambda}, \hat{k}(\bar{\lambda}), 0] \cdot \begin{pmatrix} u^s_{\bar{k}}(\bar{\lambda}, \hat{k}(\bar{\lambda}), 0) \\ v^s_{\bar{k}}(\bar{\lambda}, \hat{k}(\bar{\lambda}), 0) \\ 1 \end{pmatrix} d\tau \\ &=: \; \hat{M}(\bar{\lambda}). \end{aligned} \tag{5.29}$$

At $\bar{\lambda} = 0$ we have the identities $\hat{M}(0) = 0$ due to $(u^s_{\bar{k}}, v^s_{\bar{k}})(0,0,0) = 0$ (cf. (5.22)) and $F_{\bar{k}}[\hat{u}(\tau, 0), 4, 0, \hat{k}(0), 0] = 0$ due to (5.2). Further differentiation at $\bar{\lambda} = 0$ shows after some calculations

$$\begin{aligned} \hat{M}'(0) \;&=\; -\int_{-\infty}^{\infty} \psi^T(\tau, 0) \cdot \frac{d}{d\bar{\lambda}} \, F_{\bar{k}}[\hat{u}(\tau, \bar{\lambda}), \hat{v}(\bar{\lambda}), \bar{\lambda}, \hat{k}(\bar{\lambda}), 0]_{|\bar{\lambda}=0} \; d\tau \\ &=\; -b_2 \cdot \int_{-\infty}^{\infty} \dot{\bar{u}}_1^2(\tau, 4) \; d\tau \;\neq\; 0 \; . \end{aligned} \tag{5.30}$$

According to (5.16) this yields the surfaces

$$\bar{k} \;=\; \bar{k}^+(\bar{\lambda}, \bar{\epsilon}), \quad 0 \le \bar{\epsilon} \le \bar{\epsilon}_0(\bar{\lambda}) \qquad \text{and} \qquad \bar{k} \;=\; \bar{k}^-(\bar{\lambda}, \bar{\epsilon}), \quad -\bar{\epsilon}_0(\bar{\lambda}) \le \bar{\epsilon} \le 0 \tag{5.31}$$

of homoclinic orbits which branch off from the curve $[u, v, \bar{\lambda}, \bar{k}, \bar{\epsilon}] = [\hat{u}(\tau, \bar{\lambda}), \hat{v}(\bar{\lambda}), \bar{\lambda}, \hat{k}(\bar{\lambda}), 0]$ for $0 < |\bar{\lambda}| \ll 1$. Hence we can extend diagram (b) in Fig.10 as depicted in diagram (c). Note that in general we can not expect $\bar{k}^+(\bar{\lambda}, \bar{\epsilon})$ and $\bar{k}^-(\bar{\lambda}, \bar{\epsilon})$ to form a smooth surface along $\hat{k}(\bar{\lambda})$. The precise behavior of $\bar{\epsilon}_0(\bar{\lambda})$ remains unknown as $\bar{\lambda}$ tends to zero. The surfaces show again a symmetry given by $\bar{k}^+(\bar{\lambda}, \bar{\epsilon}) = \bar{k}^-(-\bar{\lambda}, -\bar{\epsilon})$ and we can restrict to $\bar{k}^+(\bar{\lambda}, \bar{\epsilon})$.

The different surfaces $\bar{\lambda}^{\pm}(\bar{k}, \bar{\epsilon})$ and $\bar{k}^{\pm}(\bar{\lambda}, \bar{\epsilon})$ of homoclinic orbits in diagram (c) of Fig.10 are presumably parts of a common surface of homoclinic orbits as indicated by broken lines. Numerical calculations strongly confirm this conjecture. For closing analytically the gaps between the different surfaces it would be necessary to generalize the bifurcation result in [3].

The back transformation

In this section we transform the results obtained for the blown–up system (5.2) back to the system (3.7); i.e. we interpret the surfaces from Fig.10 within the (λ, k, ϵ)–unfolding space of our singularly perturbed Bogdanov point using the scaling transformation (5.1). Essentially this yields the hatched upper part of the surface of homoclinic orbits in Fig.8.

First we indicate the transformation of $\bar{\lambda}^+(\bar{k}, \bar{\epsilon})$ in case of $b_2 \neq 0$ which occurs at a singularly perturbed Bogdanov point with a generic unfolding. According to (5.26)–(5.28) we obtain

$$\bar{\lambda}^+(\bar{k}, \bar{\epsilon}) \;=\; \frac{35}{4} \cdot \frac{1}{\gamma - 7b_2\bar{k}} \cdot \bar{\epsilon} \;+\; O(\bar{\epsilon}^2), \qquad \bar{\epsilon} \in [0, \bar{\epsilon}_0(\bar{k})], \qquad \bar{k} \neq \bar{k}(4) \tag{5.32}$$

or equivalently

$$\bar{\epsilon}^+(\bar{k}, \bar{\lambda}) \;=\; \tfrac{4}{35}(\gamma - 7b_2\bar{k}) \cdot \bar{\lambda} \;+\; O(\bar{\lambda}^2), \qquad \bar{k} \neq \bar{k}(4) \tag{5.33}$$

where $\bar{\epsilon}^+(\bar{k}, \cdot)$ denotes the inverse function of $\bar{\lambda}^+(\bar{k}, \cdot)$ and $\bar{\lambda}$ is chosen according to

$$\bar{\lambda} \;\in\; \left\{ \begin{array}{lll} [0,\ \bar{\lambda}_0(\bar{k})] & \text{in case of} & \gamma - 7b_2\bar{k} > 0 \\[2ex] [-\bar{\lambda}_0(\bar{k}),\ 0] & \text{in case of} & \gamma - 7b_2\bar{k} < 0 \end{array} \right\} \tag{5.34}$$

with $0 < \bar{\lambda}_0(\bar{k}) \ll 1$ and $\bar{\lambda}_0(\bar{k}) \to 0$ as $\bar{k} \to \pm\infty$ or as $\bar{k} \to \bar{k}(4)$. Then recalling the scaling transformation (5.1), the system (3.7) has homoclinic orbits at parameter values

$$(\epsilon,\ \lambda,\ k) \;=\; (\ \tfrac{4}{35}c_4(\gamma - 7b_2\bar{k}) \cdot \bar{\lambda}^4 \;+\; O(\bar{\lambda}^5), \quad c_5 \cdot \bar{\lambda}^2, \quad c_6\bar{k} \cdot \bar{\lambda}^2\ ) \tag{5.35}$$

with $\bar{k} \in \mathbb{R} \setminus \{\bar{k}(4)\}$ and $\bar{\lambda}$ chosen according to (5.34). For fixed $\bar{k}$ we obtain a curve in the (λ, k, ϵ)–space parametrized by $\bar{\lambda}$. The projection of this curve onto the (λ, k)–plane forms the straight line

$$k \;=\; \frac{c_6}{c_5}\,\bar{k} \cdot \lambda\,, \qquad \lambda \in \left\{ \begin{array}{lll} [0,\ c_5\bar{\lambda}_0^2(\bar{k})] & \text{in case of} & c_5 > 0 \\[2ex] [c_5\bar{\lambda}_0^2(\bar{k}),\ 0] & \text{in case of} & c_5 < 0 \end{array} \right\}. \tag{5.36}$$

In contrast to this the projection of the curve onto the (λ, ϵ)–plane yields the parabola

$$\epsilon \;=\; \frac{4}{35}\,\frac{c_4}{c_5^2}\,(\gamma - 7b_2\bar{k}) \cdot \lambda^2 \;+\; O(\lambda^2\sqrt{\lambda})\,. \tag{5.37}$$

During variation of $\bar{k} \in (-\infty, \bar{k}(4))$ and $\bar{k} \in (\bar{k}(4), \infty)$ we obtain the surfaces [1] and [4] as indicated in diagram (b) of Fig.11. These two surfaces represent parts of the hatched upper part in Fig.8. Remember that Figures 8 and 11 show the (λ, k, ϵ)–unfolding space of a singularly perturbed Bogdanov point with a generic unfolding.

The outer and inner border lines of the surfaces [1] and [4] show the limiting behavior

$$\frac{\lambda}{k} \;=\; \frac{c_5\bar{\lambda}_0^2(\bar{k})}{c_6\bar{\lambda}_0^2(\bar{k}) \cdot \bar{k}} \;=\; \frac{c_5}{c_6} \cdot \frac{1}{\bar{k}} \;\to\; \left\{ \begin{array}{lll} 0 & \text{as} & \bar{k} \;\to\; \pm\infty \\[2ex] \dfrac{c_5}{c_6} \cdot \dfrac{1}{\bar{k}(4)} & \text{as} & \bar{k} \;\to\; \bar{k}(4) \end{array} \right\}. \tag{5.38}$$

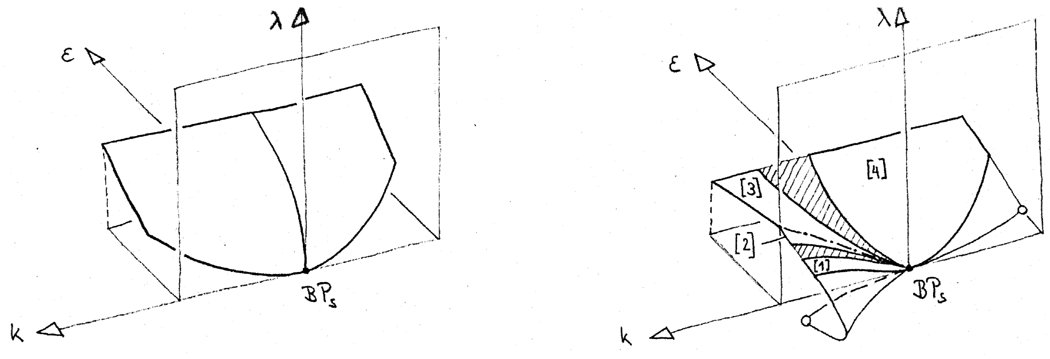

(a) (b)

Figure 11: The different surfaces of homoclinic orbits of the pretransformed system (3.7), (a) $b_2 = 0,\ \gamma \neq 0$, (b) $b_2 \neq 0$.

In particular we have $\lambda/k = o(1)$ if we approach the origin along the outer border lines. Along the inner border lines we approach the dotted curve of singularly perturbed homoclinic orbits given by

$$k \;=\; \frac{c_6}{c_5}\,\lambda\cdot\hat{k}(\sqrt{\lambda/c_5}) \;=:\; k^{Ho}(\lambda) \qquad \text{with} \qquad k^{Ho}_{\lambda}(0) \;=\; \frac{c_6}{c_5}\cdot\bar{k}(4) \;=\; \frac{c_6}{c_5}\cdot\frac{\gamma}{7b_2}\,. \tag{5.39}$$

In case of $\bar{k}(4) = 0$ the curve is tangentially touching the λ–axis. This situation occurs in the FitzHugh–Nagumo equation where the singularly perturbed homoclinic orbits are exactly positioned on the $a = \lambda$–axis as shown in diagram (b) of Fig.1. This special case is treated in detail in [3].

Next we consider $\bar{\lambda}^+(\bar{k}, \bar{\epsilon})$ in case of $b_2 = 0,\ \gamma \neq 0$ (cf. diagram (a) in Fig.10). In this situation we can choose $\bar{k} \in \mathbb{R}$ and obtain a unique surface in the (λ, k, ϵ)–parameter space as indicated in diagram (a) of Fig.11. More precisely there exist homoclinic orbits at parameter values

$$(\epsilon,\ \lambda,\ k) \;=\; (\ \tfrac{4}{35}c_4\gamma\cdot\bar{\lambda}^4 \;+\; O(\bar{\lambda}^5),\quad c_5\cdot\bar{\lambda}^2,\quad c_6\bar{k}\cdot\bar{\lambda}^2\ ) \tag{5.40}$$

with $\bar{k} \in \mathbb{R}$ and $\bar{\lambda}$ chosen according to

$$\bar{\lambda} \;\in\; \left\{ \begin{array}{lll} [0,\ \bar{\lambda}_0(\bar{k})] & \text{in case of} & \gamma > 0 \\ & & \\ [-\bar{\lambda}_0(\bar{k}),\ 0] & \text{in case of} & \gamma < 0 \end{array} \right\}$$

with $\bar{\lambda}_0(\bar{k}) \to 0$ as $\bar{k} \to \pm\infty$.

In principle the transformation of the two surfaces $\bar{k}^+(\bar{\lambda}, \bar{\epsilon}),\ 0 < \bar{\lambda} \ll 1$ and $\bar{k}^+(\bar{\lambda}, \bar{\epsilon}),\ -1 \ll \bar{\lambda} < 0$ from diagram (c) in Fig.10 works along the same lines as the transformation of $\bar{\lambda}^+(\bar{k}, \bar{\epsilon})$, so we omit the details. We obtain the surfaces [2] and [3] in diagram (b) of Fig.11.

According to the theory we can only guarantee the surfaces [1], [2] and [3], [4] separated by the hatched gaps. But these gaps can be closed and there is one common surface according to numerical calculations. This surface intersects the (λ, k)–plane along the dotted curve $k^{Ho}(\lambda)$ of singularly perturbed homoclinic base points (cf. (5.39)). In general we cannot expect the surface to be smooth with respect to ϵ along this curve. Note that during variation of $b_2 \to 0$ the curve tends to the k–axis and we approximate diagram (a).

Using the derivatives in (5.39), (4.9) and the transformations (3.6), (5.1), (5.3) it is now possible to draw a complete picture of the singularly perturbed points of the pretransformed system (3.7) and the original system (2.1). First, we obtain from (5.39) singularly perturbed homoclinic base points at $[\lambda, k] = [\lambda, k^{Ho}(\lambda)]$ with $0 < \lambda \ll 1$ in case of $c_5 = -f^0_{2x_1x_1} g^0_{x_1} / g^0_\lambda > 0$ and with $-1 \ll \lambda < 0$ in case of $c_5 < 0$. The derivative at $\lambda = 0$ is given by $k^{Ho}_\lambda(0) = c_6\gamma/(c_5 7 b_2)$. The singularly perturbed saddle-nodes occur at $[\lambda, k] = [0, k]$, $0 < |k| \ll 1$ and finally we obtain singularly perturbed Hopf points $k^H(\lambda)$ with $0 < \lambda \ll 1$ in case of $\bar{H}'(0) = f^0_{2x_1x_1} g^0_\lambda / g^0_{x_1} > 0$ and with $-1 \ll \lambda < 0$ in case of $\bar{H}'(0) < 0$. The corresponding derivative $k^H_\lambda(0)$ at $\lambda = 0$ is given by (4.9). Note that $\bar{H}'(0) \cdot c_5 = -(f^0_{2x_1x_1})^2 < 0$ so that the singularly perturbed Hopf points and the singularly perturbed homoclinic orbits exist on different sides of the k–axis which represents the singularly perturbed saddle–nodes.

Qualitatively we obtain diagram (a) in Fig.1 with $(p_1, p_2) = (\lambda, k)$. Here we chose $c_5 > 0$, $k^{Ho}_\lambda(0) > 0$ and $k^H_\lambda(0) < 0$ which occurs in case of the model equation (1.3). The singularly perturbed points in the (p_1, p_2)–parameter space of the original system (2.1) are obtained by diffeomorphically deforming the curves according to the transformation (3.6).

In case of the Fitzhugh–Nagumo equation (1.2) we obtain diagram (b) in Fig.1; i.e. the singularly perturbed homoclinic orbits and the singularly perturbed Hopf points are both located on the a–axis. In particular they form a smooth curve at the singularly perturbed Bogdanov point at $a = 0$. This is a degenerate situation which results from the fact that the central u–system $\dot{u}_1 = u_2$, $\dot{u}_2 = -u_1^2 + u_1^3$ has a Bogdanov point in a Hamiltonian system.

In general we obtain this degenerate case if a certain normal form coefficient of the central system vanishes, as can be seen by the following argument. At $(\lambda, k, \epsilon) = 0$ the x–part of the system (3.7) assumes the following form after performing a standard normal form transformation

$$\begin{aligned} \dot{x}_1 &= x_2 + O(|x|^3) \\ \dot{x}_2 &= \tfrac{1}{2} f^0_{2x_1x_1} \cdot x_1^2 + \mathrm{tr}_{x_1}(f_x)^0 \cdot x_1 x_2 + O(|x|^3) . \end{aligned} \tag{5.41}$$

Hence the Bogdanov point is nondegenerate iff $f^0_{2x_1x_1} \neq 0$ and $\mathrm{tr}_{x_1}(f_x)^0 \neq 0$ (cf. [14]). The first inequality is valid according to (3.8). Concerning the second inequality the equations (5.39) and (4.9) yield the equivalence

$$k^{Ho}_\lambda(0) \neq k^H_\lambda(0) \qquad \Longleftrightarrow \qquad \mathrm{tr}_{x_1}(f_x)^0 \neq 0 ; \tag{5.42}$$

i.e. generically we have $\mathrm{tr}_{x_1}(f_x)^0 \neq 0$ and the singularly perturbed Bogdanov point causes curves of singularly perturbed homoclinic orbits, singularly perturbed saddle–nodes and singularly perturbed Hopf points which meet transversally at the origin. The corresponding (λ, k, ϵ)–unfolding diagram is depicted in diagram (a) of Fig.2. When approaching the degenerate case $\mathrm{tr}_{x_1}(f_x)^0 = 0$ of a nontransversal intersection the precise behavior of the surfaces in Fig.2 diagram (a) is not clear.

5.2 Numerical results

We close the paper by numerically continuing the surface of homoclinic orbits to the border line indicated by the open circles in Fig.2, Fig.8 and Fig.11. This is done for the model

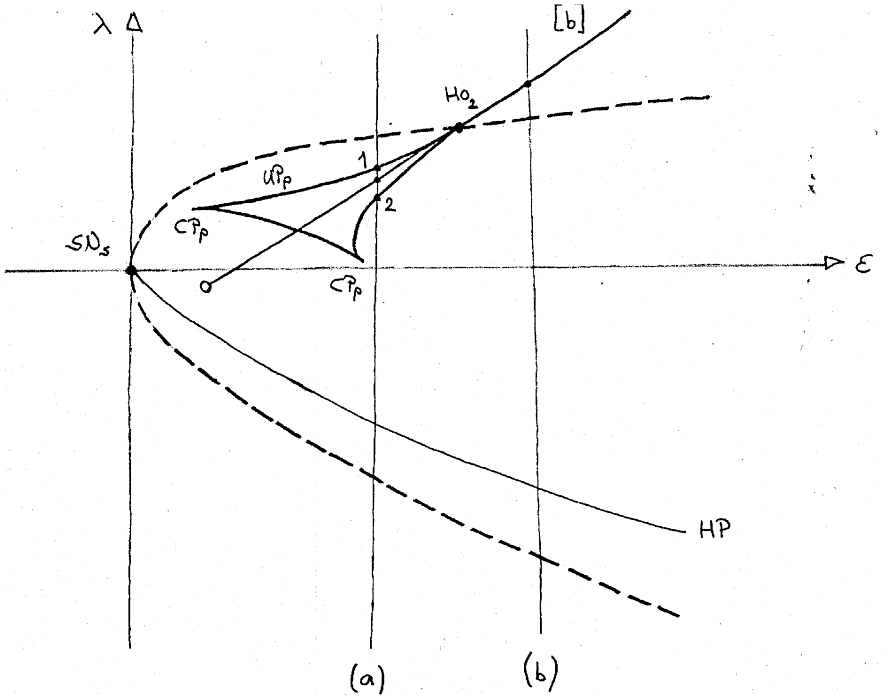

Figure 12: The (λ, ϵ)–section through Fig.2 for fixed $-1 \ll k < 0$.

equation (1.3). With $(p_1, p_2) = (\lambda, k)$ and for fixed $-1 \ll k < 0$ the (λ, ϵ)–section through Fig.2 yields the structures depicted in Fig.12.

On the left side of the broken line we obtain three real eigenvalues at the stationary point $(u_1, u_2, v) = (\lambda, 0, -\lambda^2)$ whereas on the right side a conjugate–complex pair of eigenvalues $(\rho \pm i\omega) \in \mathbb{C}$ coexists with one real eigenvalue $\kappa \in \mathbb{R}$ with $|\kappa| > |\rho|$. Consequently, the homoclinic orbits Ho turn into homoclinic orbits of Shilnikov type [14] when crossing the broken line at the degenerate homoclinic orbit Ho_2 during variation of ϵ towards zero. Ho_2 is a well known codimension-two homoclinic bifurcation (see [5] for numerical and theoretical results). Fig.13 shows the corresponding bifurcation diagrams along the λ–sections (a) and (b) in Fig.12.

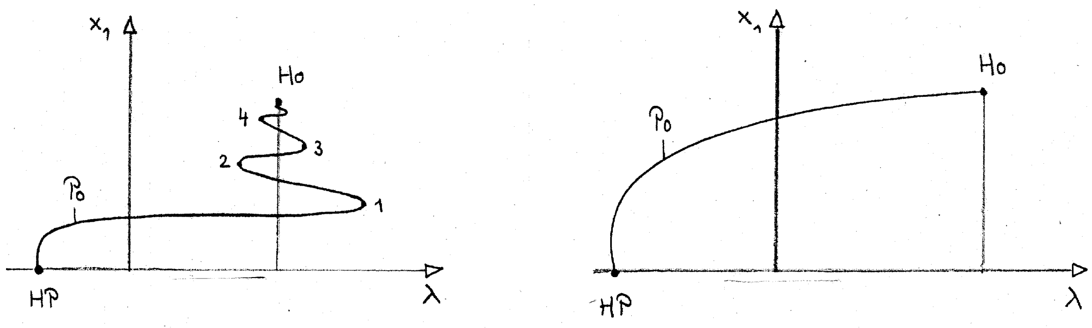

(a) (b)

Figure 13: The bifurcation diagrams along the λ–sections (a) and (b) in Fig.12.

In particular we obtain in the left diagram an infinite sequence 1,2,3,4,... of periodic limit points with respect to λ. The first two limit points 1 and 2 are also marked along the line (a) in Fig.12. Now the numerical continuation of these points within the (λ, ϵ)–space of Fig.12 yields the closed curve UP_p of periodic limit points; i.e. the limit points 1 and 2 are connected by a curve that emanates from the degenerate homoclinic orbit Ho_2 and which contains additionally the two cusp points CP_p of periodic orbits. These cusp points arise by the coalescence of two limit points.

An analogous connection exists between the next two limit points 3 and 4 in Fig.13 and so forth. Hence we expect that the (λ, ϵ)–unfolding diagram in Fig.12 can be extended by an infinite sequence of closed curves which approach the curve of homoclinic orbits Ho as indicated in Fig.14.

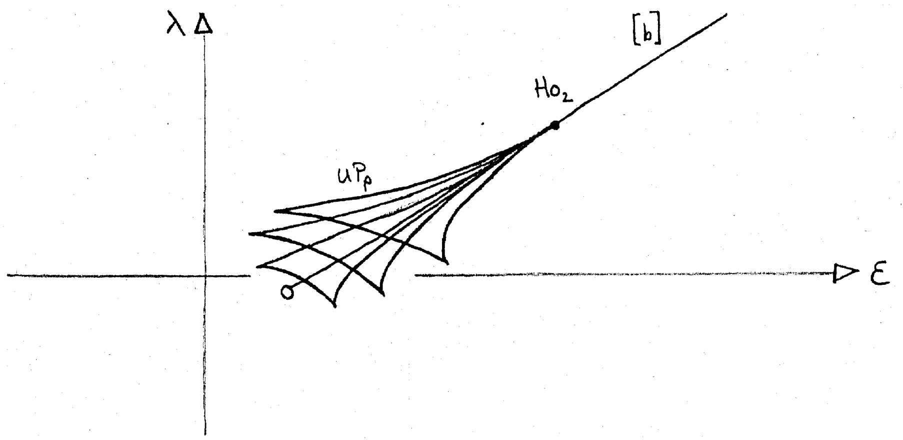

Figure 14: Closed curves of periodic limit points in the (λ, ϵ)–plane.

Unfortunately, this observation does not clarify the behavior of the homoclinic orbits near the open circle. However, numerical calculations suggest that a duck like blow–up occurs as indicated in diagram (d) of Fig.2; i.e. the homoclinic orbits of Shilnikov–type blow–up along the continuum of stationary points $v = -u_1^2$ which exists at $\epsilon = 0$. These blow–up phenomena typically occur in an exponentially small strip that is hardly accessible to numerical calculations.

Note that within the complete (λ, k, ϵ)–unfolding space of the model equation (1.3) we obtain a curve of open circles that passes through the singularly perturbed Bogdanov point at $k = 0$ (cf. Fig.2). The (k, ϵ)–dependency seems to be of cubic order; i.e. we expect $k(\epsilon) = O(\epsilon^3)$ near the singularly perturbed Bogdanov point.

Acknowledgement: This paper represents an extended part of the authors thesis. It was supported by the DFG–Schwerpunktprogramm "Ergodentheorie, Analysis und effiziente Simulation dynamischer Systeme" and was carried out during a four–month visit at the University of Bielefeld and a seven-month visit at the University of Tübingen. The author wishes to express his thanks to Prof. W.–J. Beyn, Prof. E. Bohl and Prof. K. P. Hadeler.

References

[1] Arnold V. I., Afrajmovich V. S., Il'yashenko Y. S., Shil'nikov L. P. (1994): Dynamical Systems V: Bifurcation Theory. Springer.

[2] Beyn W.–J. (1994): Numerical analysis of homoclinic orbits emanating from a Takens-Bogdanov point. IMA J. Numer. Anal. **14**, 381-410.

[3] Beyn W.–J., Stiefenhofer M. (1997): A direct approach to homoclinic orbits in the fast dynamics of singularly perturbed systems. DFG–Schwerpunktprogramm: Dynamik, Analysis, effiziente Simulation und Ergodentheorie. Preprint No. **15**, to appear in Journal of Dynamics and Differential Equations.

[4] Casten R. G., Cohen H., Lagerstrom P. A. (1975): Perturbation analysis of an approximation to the Hodgkin–Huxley theory. Quart. Appl. Math. **32**, 365-402.

[5] Champneys A. R., Kuznetsov Y. A. (1994): Numerical detection and continuation of codimension-two homoclinic bifurcations. Internat. J. Bifur. Chaos Appl. Sci. Engrg. **4**, 785-822.

[6] Chow S.–N., Hale J., Mallet–Paret J. (1980): An example of bifurcation to homoclinic orbits. J. Differential Equations **37**, 351-373.

[7] Diener M. (1981): Étude générique des canards. IRMA, Strasbourg.

[8] Doedel E.J., Kernevez J.P. (1986): AUTO – Software for continuation and bifurcation problems in ordinary differential equations. Appl. Math. Technical Report, CALTECH.

[9] Dumortier F., Roussarie R. (1996): Canard Cycles and Center Manifolds. AMS Vol. **121**, Nr. **577**.

[10] Eckhaus W. (1983): Relaxation oscillations including a standard chase on french ducks. In: Lecture notes in Mathematics **985**, 449-494, Springer.

[11] Fenichel N. (1979): Geometric singular perturbation theory for ordinary differential equations. J. Differential Equations **31**, 53–98.

[12] Gibson C. G. (1979): Singular points of smooth mappings. Pitman

[13] Martiel J.–L., Goldbeter A. (1987): A model based on receptor desensitization for cyclic AMP signalling in Dictyostelium cells. Biophs. J. **52**, 802–828.

[14] Guckenheimer J., Holmes P. (1990): Nonlinear Oscillations, Dynamical Systems , and Bifurcations of Vector Fields (3rd printing). Appl. Math. Sci. **42**, Springer.

[15] Hastings S. P. (1982): Single and multiple pulse waves for the FitzHugh–Nagumo equations. SIAM J. Appl. Math. **42**, 247–260.

[16] Haken H. (1978): Synergetics. An introduction. Springer.

[17] Jones C. K. R. T., Kopell N. (1994): Tracking invariant manifolds with differential forms in singularly perturbed systems. J. Differential Equations **108**, 64–88.

[18] Koper M. (1995): Bifurcations of mixed–mode oscillations in a three–variable autonomous Van der Pol–Duffing model with a cross–shaped phase diagram. Physica **D80**, 72–94.

[19] Kuznetsov Y. (1995): Elements of Applied Bifurcation Theory. Springer, New York.

[20] Murray J.D. (1989): Mathematical Biology. Springer, Berlin, New York.

[21] NAG (1983): Numerical Algorithms Group, Oxford.

[22] Palmer K. J. (1984): Exponential dichotomies and transversal homoclinic points. J. Differential Equations **55**, 225-256.

[23] Shub M. (1987): Global Stability of Dynamical Systems. Springer.

[24] Stiefenhofer M. (1995): Singuläre Störung und Verzweigung bei Schleimpilzen. PhD Thesis, University of Konstanz, Hartung–Gorre Verlag, Konstanz.

[25] Stiefenhofer M. (1996): Singular perturbation with limit points in the fast dynamics. DFG–Schwerpunktprogramm: Dynamik, Analysis, effiziente Simulation und Ergodentheorie. Preprint No. **61**, to appear in ZAMP.

[26] Stiefenhofer M. (1996): Singular perturbation with Hopf points in the fast dynamics. DFG–Schwerpunktprogramm: Dynamik, Analysis, effiziente Simulation und Ergodentheorie. Preprint No. **59**, to appear in ZAMP.

[27] Szmolyan P. (1991): Transversal heteroclinic and homoclinic orbits in singular perturbation problems. J. Differential Equations **92**, 252–281.

[28] Vasil'eva A. B. (1963): Asymptotic behaviour of solutions to certain problems involving nonlinear differential equations containing a small parameter multiplying the highest derivatives. Russian Math. Surveys **18**, 13–84.